

AN ASSESSMENT OF SELF-ORGANIZED CRITICALITY WITHIN A MOUNTAIN
RIVER SYSTEM

THESIS

Presented to the Graduate Council of
Texas State University – San Marcos
in Partial Fulfillment of
the Requirements

for the Degree

Master of Science

by

Jane B. Heath, B.A.

San Marcos, Texas
August 2006

ACKNOWLEDGEMENTS

I would like to thank Dr. Mark Fonstad and Dr. Andrew Marcus for co-authoring an article that I read my first semester in graduate school for a class. Self-Organized Criticality in River Systems re-ignited my interest in geography and led me to the world of systems analysis. I would, above all, like to thank Dr. Fonstad for providing unbending enthusiasm, support, and the necessary resources to allow me to conduct my fieldwork in majestic Silverton, Colorado. I would also like to thank my committee members Dr. David Butler and Dr. Andrew Marcus for being so patient and enthusiastic about this thesis. They are exceptional scholars.

Many thanks also must go to the Summer '05 Silverton Field Crew: Mindy Conyers and Bernadette Marion. These women were indefatigable at assisting me, never complained, and always insisted that they liked it even as they were duct taping their blisters in the thunderstorms. This fieldwork would have never been completed without the solidarity of this group and the sheer love of geography in their hearts. Not to mention Colorado Microbrew.

I would also like to thank my family, Diane, Michael, and Jenny, who have been so encouraging and continue to support and nourish my life choices. Lastly, I would like to thank my husband Mike for always provide a warm home that even on my worst days makes me feel like a queen. This manuscript was submitted on April 13, 2006.

TABLE OF CONTENTS

	Page
ACKNOWLEDGEMENTS.....	iii
LIST OF TABLES.....	vi
LIST OF FIGURES.....	vii
CHAPTER	
I. INTRODUCTION.....	1
II. LITERATURE REVIEW.....	3
• Concepts of Self-Organized Criticality	
• SOC in River Meandering	
• Mountain Stream Characteristics	
• Fluvial Wood Impacts on Mountain Streams	
• Field Estimation Techniques	
• Summation	
III. STUDY AREA.....	18
IV. METHODOLOGY.....	23
• Introduction	
• Data Collection	
• Data Analysis	
V. RESULTS.....	30
• Introduction	
• The Spatial Distribution of Bank Failures	
• The Magnitude and Frequency of Bank Failures	
• Fluvial Wood and its Effects on Bank Failure Power Laws	
VI. DISCUSSION AND CONCLUSION.....	43

- Discussion
- Conclusion

APPENDIX I.....	49
APPENDIX II.....	130
APPENDIX III.....	174
APPENDIX IV.....	178
WORKS CITED.....	182

LIST OF TABLES

Table	Page
1. Upper Animas Watershed Characteristics	20
2. Bins of Bank Failure Classes for Mineral Creek	31
3. Bins of Bank Failure Classes for Cement Creek	31
4. Power law statistics for Bank Failure Occurrences	38
5. Bins of Bank Failure Classes with Fluvial Wood for Cement Creek.....	39
6. Bins of Bank Failure Classes with Fluvial Wood for Mineral Creek.....	39
7. Comparison of Tau Slopes for Bank Failure with and without Fluvial Wood	40

LIST OF FIGURES

Figure	Page
1. Sandpile Toy Model.....	6
2. Illustration of the Toppling Process.....	7
3. Location map of the Upper Animas Watershed	19
4. General Geology of Upper Animas Watershed	21
5. Location of Silverton, CO and Streams of Interest	22
6. Location of Waypoints Bordering Each Reach in Study Area.....	24
7. Delineated Line Showing the Extent of the Bank Failure within a Photograph in AutoCad	26
8. Example of distance to focal point determination	27
9. Fluvial Wood in Channel of Mineral Creek.....	29
10. Left Bank Failure Downstream Distribution for Cement Creek	32
11. Right Bank Failure Downstream Distribution for Cement Creek	32
12. Left Bank Failure Downstream Distribution for Mineral Creek	33
13. Right Bank Failure Downstream Distribution for Mineral Creek	33
14. Locations of Left Bank Failure Distribution for Mineral and Cement Creeks.....	35
15. Locations of Right Bank Failure Distribution for Mineral and Cement Creeks.....	36
16. Power Law Distributions of Presence of Fluvial Wood in Cement Creek.....	41

17. Power Law Distributions of Presence of Fluvial Wood in Mineral
Creek 42

CHAPTER I

INTRODUCTION

Research in nonlinear systems dynamics has grown rich and layered with the relatively recent emergence of fresh new insights that explain these phenomena outside of the reductionist or narrative context. Self-organized criticality (SOC), a concept developed by Per Bak, a Danish physicist, in the 1980s has continued to intrigue and underpin much of contemporary systems analysis and modeling of physical systems in geomorphology. Its roots lie in the idea that large-scale behavior in nature obeys fundamental laws that describe an array of systems from forest fires to evolution (Bak and Paczuski, 1996). This paper, however, specifically is interested in the intrinsic spatial variability of riverbank instability that has been theorized to obey a power law describing the magnitude and frequency distribution of bank failure.

The purpose of this assessment is to answer the research questions, “Does the magnitude and frequency of riverbank failure in mountain streams obey a power law?” and, “Is there a correlation between the slope of the power law with effective wood in and around the fluvial system?” The answers lie in an observational field study empirically testing the magnitude and frequency of mass bank erosion and accompanying fluvial wood, defined as any wood located within, or impeding, the channel regardless of source. The field data subsequently are plotted and analyzed statistically to illustrate the

potential occurrence of power laws indicating the necessary behavior to maintain a critical state. The hypotheses to be tested are (a) power laws will emerge from the magnitude and frequency of bank failure events measured in the field, and (b) the existence of fluvial wood in areas of bank failure has a stabilizing effect causing greater power law slopes.

The significance of this approach to interpretation of bank erosion processes and behavior is practical as much as it is unique. Rivers are active systems that are continually changing and taking new shape. It is necessary to try and predict the dynamics of these system processes for stability of future developments as well as restoration efforts.

CHAPTER II

LITERATURE REVIEW

Concepts of Self-Organized Criticality

1/f Noise

Researchers interested in the analysis of physical systems have struggled with the existence of “1/f noise”, sometimes referred to as “flicker noise” or “pink noise” in nature, which refers to the fluctuations of a system over time that have a spectral, or power, density inversely proportional to the frequency (Gilden *et al.*, 1995). This type of noise is reflected by correlations that extend over broad ranges of time, indicating some sort of inter-relation and cooperation between events (Bak *et al.*, 1988). Its seemingly ubiquitous appearance in systems ranging from evolution to the Internet is puzzling, and continues to be examined by researchers from many fields. More than fifteen years ago, Per Bak, Chao Tang, and Kurt Wiesenfeld argued and revealed through quantification the theory of SOC as an explanation of 1/f noise (Bak *et al.*, 1987). They hold that 1/f noise is the dynamical response to small random perturbations of minimally stable structures. Several models were employed to support this concept with the results being the existence of a power-law distribution of length and time scales validating their idea of SOC (Bak *et al.*, 1987).

Fractal Patterns

Fractal structures in combination with power law distributions abound in many geomorphic systems. Fractals are a mathematical concept that explains the existence of irregular shapes that maintain their form over a range of scales (Rodríguez-Íturbe and Rinaldo, 1997). Fractal geometry contains self-similarity and consequently scale invariance. The result of this invariance and complexity is that through scrupulous examination of a self-similar system at different scales, more and more complex structures that are identical to the larger structures found at a broader scale will be revealed (Rodríguez-Íturbe and Rinaldo, 1997). The ‘fractal dimension’, a noninteger between the dimension of the constituting elements and the embedded dimension, is the key property from which the spatial self-similar pattern arises (Baas, 2002; Bolliger *et al.*, 2003).

Fractals are abundant in earth systems, and therefore have been studied in relation to geomorphic phenomena for years. One essential component of fractal patterns is the power-law structures that make up the logged magnitude and frequency distributions that characterize their geometric shape. The fractal dimension is the exponent of power-law scaling (Stølum, 1998). Power laws indicate that systems may experience events randomly of all sizes, but are characterized by intermittent bursts, or punctuated equilibrium (Rodríguez-Íturbe and Rinaldo, 1997). It could be argued that fractals are the minimally stable states that are derived from dynamic processes that stop precisely at the critical phase (Bak *et al.*, 1987).

The Sandpile Paradigm

One of the models created, the sandpile model, has become a prevailing model utilized to explain and test SOC. Essentially the model represents a situation of a table where there is a slow continuous spout of sand being added on the center, also allowing it to fall off the edges. The amount of sand that flows off of the pile is the quantity that exhibits the $1/f$ noise (Bak *et al.*, 1988). The initial flat state is that of general equilibrium with the lowest amount of energy, however, as the pile becomes steeper, small avalanches begin to occur. Addition of grains may cause local disturbances or avalanches, yet nothing happens outside of the region and the disturbance is proportional to the event and contingency is irrelevant. Eventually, however, after enough sand is added, the pile reaches a balanced state, where the amount of sand falling off of the edges of the table more or less equals the amount of sand remaining with avalanches having occurred of all sizes. It is at this state that the pile has transformed from individual grains controlling their own local dynamics to one with a globally complex system where an individual grain has the potential to disturb the whole pile (Bak and Paczuski, 1996).

Relatively few other controlled experiments to test SOC exist, but one that does tests the dynamics on a 3D pile of rice (Aegerter *et al.*, 2004). This test was done in order to measure the gap of the avalanches and the evolution of avalanche size and distributions. Results adhere to the principles of the original sandpile model, and better understanding of the evolution to the critical state was found (Aegerter *et al.*, 2004).

Several other experiments, however, utilizing 2D modeling are found with more frequency, such as the Hergarten and Neugebauer cellular automata model of two variables (Hergarten and Neugebauer, 2000). This model is a generalization of the

original sandpile and still maintains power-law distribution (Hergarten and Neugebauer, 2000). Figure 1 demonstrates a toy sandpile model and the rules that cause avalanches to occur. Addition of sand is continued onto a cell until that cell contains more than three grains of sand. When the fourth grain is added, each of the grains topples to its immediate four downhill neighbors. These simple rules are the basis for the majority of spatial models constructed to test SOC.

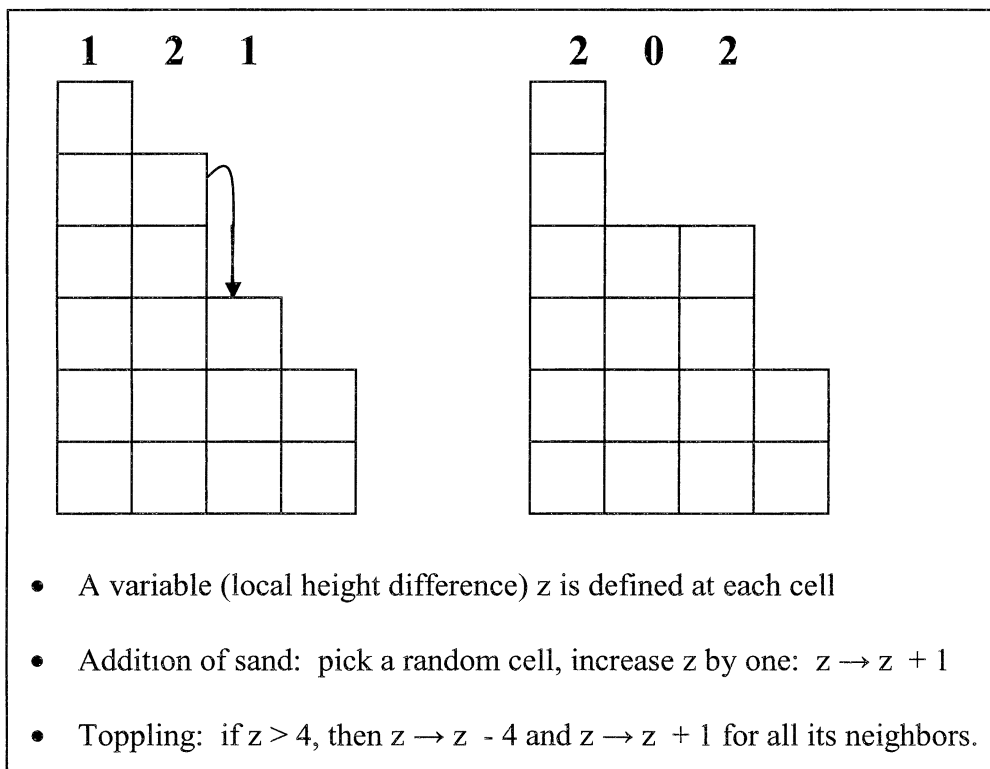


Figure 1. Sandpile Toy Model.

Figure 2 illustrates the toppling process of the sandpile model. The numbers represent the number of grains of sand that are present on each cell. When the number reaches four, the grains disperse and the cell returns to zero grains. This process reveals

the dynamics of local avalanches and simplifies the behavior of processes of systems theorized to have SOC characteristics.

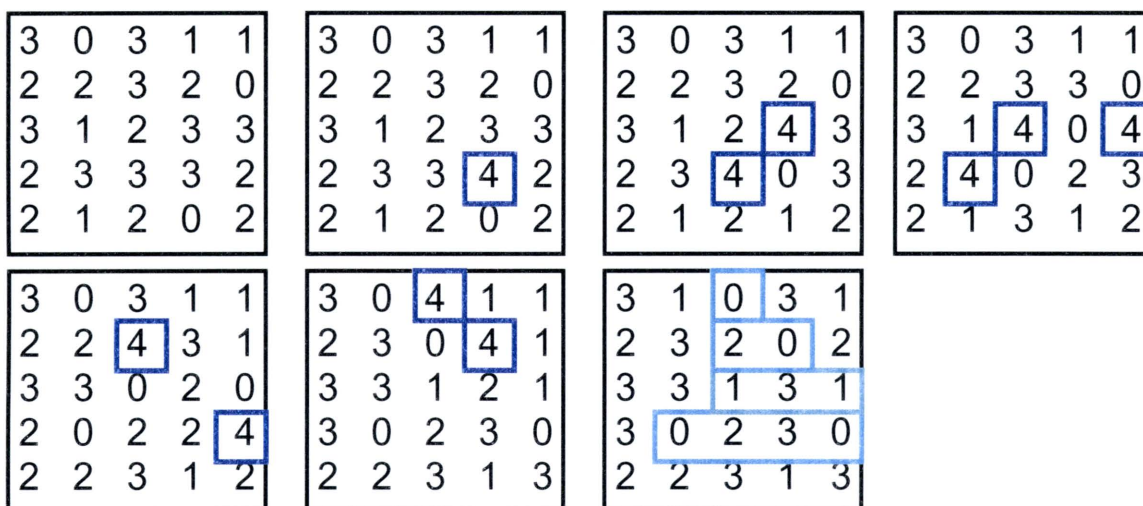


Figure 2. Illustration of the Toppling Process. Each number represents the number of grains contained in each cell. The darker squares highlight the cells with 4 grains of sand, the maximum amount before an avalanche, while the lighter squares highlight the cells with added grains and subtracted grains after the toppling process occurs.

Landslides

Although controlled experiments testing SOC are somewhat limited, numerous studies of observed geomorphic power-law through space processes exist. For example, there are a multitude of similarities between the sandpile model and landslides. It should be noted, however, that actual landslides have depth as well as area, rendering two-dimensional modeling only approximate (Turcotte, 1999). This assumption has been tested in CA, and indeed, the power laws of actual landslides have a significantly larger exponent than those produced in the model (Turcotte and Malamud, 2000). Turcotte and Malamud (2000) suggest possible rule revisions in order to obtain a higher amount of

accuracy in the simulations. In spite of these limitations, most research evaluating SOC and landslides draws a comparison between the sandpile model and actual landslides due to their obvious commonalities. Malamud and Turcotte (1999) compare the sandpile model with magnitude and frequency distributions of actual landslides from four geographic locations. The results for large landslides reveal power-law distributions in conjunction with the principals of SOC supporting the idea that fundamental laws prevail in nature even amid dramatic variations.

Snow Avalanches

Evidence of power laws has been found in the frequency-size distribution of snow avalanches (Birkeland and Landry, 2002; Faillettaz *et al.*, 2004). Birkeland and Landry (2002) examine two datasets of long-term observations of snow avalanches that have occurred naturally, as well as a third dataset in an area containing artificially triggered avalanches strongly influenced by human decisions. The frequency-size distributions of these avalanches are plotted and result in a strong log-linear (power) relationship. They did not, however, consider $1/f$ noise because of the lack of a continual time-series in their data (Birkeland and Landry, 2002). The implications of their results provide a theoretical approach relatively new to snow avalanches, and while they do not lay claim that they necessarily align with SOC behavior, they do share some of the same characteristics.

The research of Faillettaz *et al.* (2004) recognizes these power laws in snow avalanches, and goes further to develop a CA model of snow slab avalanches. The results of their simulations, however, yield a different interpretation of the phenomena from the Birkeland and Landry study. Their model is unique in that it incorporates the mechanics of snow slab failures defined by a definitive slab strength threshold. Also, it

does not have a healing process for broken cells and is therefore always brought to an unstable state, never reaching criticality (Faillettaz *et al.*, 2004). The results from simulations within this model are suggestive to the idea that the power-law distributions are not in correspondence to SOC, but from the emergence of avalanches in the vicinity of a breakdown point (Faillettaz *et al.*, 2004). These recent studies explore the frequency-size distribution of snow avalanches, but neither wholly investigates all of the criteria essential for them to exhibit SOC. Future research and development of robust conceptual models of avalanche dynamics will be critical in further analysis of SOC behavior in snow avalanches.

Universality

Universality is a fundamental principle in SOC systems, meaning that the key variables in large-scale systems are extremely insensitive to the details of the models that are built to describe them and are in fact shared with many other seemingly non-related systems (Bak and Paczuski, 1996). In more recent studies of SOC, it has become important to produce universality classes within these systems. Kloster, Maslov, and Tang (2001) outline necessary questions to ask about the sandpile model in order to test its sensitivity in their research. These questions include whether or not a local avalanche occurs due to the height exceeding its critical value or the slope, and secondly, if the sand is redistributed invariably in all directions during a toppling event, and finally, if the sand is redistributed deterministically or randomly during a toppling event (Kloster *et al.*, 2001).

The Critical State

Physical systems that exhibit SOC must reach a critical state of quasi-stability. In this state systems show both static and dynamic scaling (Sapozhnikov and Foufoula-Georgiou, 1996). The static scaling appears in the distribution of correlation lengths of fluctuations and exhibit scale-invariance and corresponding power-law distributions during the times of relaxation of energy and are fundamentally related (Sapozhnikov and Foufoula-Georgiou, 1996). The critical state is stabilized by the tentative order of the global system, but with local instabilities (Stølum, 1997.)

Alternative Explanations for Power Laws in Nature

A substantial amount of research on SOC in river meandering exists; however, there is a gap in the research exploring the existence of power laws as truly representing an SOC system. Although SOC was first developed with the intention of explaining power laws in nature, it is now being discovered that these power laws are not necessarily an indicator of SOC phenomena. Rather, several researchers have found power laws that exist without a critical state. Power laws exist in systems that appear to be highly complex, but upon closer inspection are highly ordered and structured, the exact opposite of SOC (Carlson and Doyle, 1999). It has been argued that complexity produces structured configurations and power laws among other characteristics, due to an optimized design for uncertainty in biological systems (Carlson and Doyle, 1999).

Other research has revealed power laws exhibited in nonconserved systems, where conservation laws were once thought to be a mechanism of SOC providing evidence that power laws may exist without the presence of SOC in some systems (Middleton and Tang, 1995).

SOC in River Meandering

Much interest exists in recent years in SOC as it relates to scale invariance in river meanders. The popular methods for approaching these concepts are through empirical data used in conjunction with simulation through 2D and 3D models. These dynamic models allow for the researcher to examine the holistic, spatiotemporal characteristics of the river meandering and geomorphic process (Stølum, 1996.) It has been argued in the past, however, that the models existing prior to the mid-nineties do not show evolution to a critical state, and therefore, modeling must be regarded with skepticism due to the extreme dynamical nature of rivers (Sapozhnikov and Foufoula-Georgiou, 1996). The science of complex systems modeling of river systems in more recent years, however, has attempted to disprove this notion and some of this research will be described below. Alternative methodologies such as the use of aerial photography and remotely sensed imagery in order to determine river behavior in relation to SOC have generally been discounted, in large part, because the data do not extend far enough in time for proper measurement, again reinforcing the need for modeling (Stølum, 1998; Hooke, 2002).

River Meandering

Meandering occurs due to the behavior of two opposing processes: those of lateral migration (flow) that cause sinuosity, and the cut-off process whereby ox-bow lakes are created. The critical link is the nonlinear negative feedback of the in-stream flow and the meander pattern partially under local geometric control (Stølum, 1996; Stølum, 1998). Meander characteristics are not stable; however, research has shown that

they tend to occupy a phase space that allows for them to be linked to the conditions that exist for that domain (Hooke, 2002).

Stølum (1997) compares the dynamical characteristics of a meandering river with those of the sandpile paradigm. Whereas the sandpile model has four instabilities, or properties that propel the system away from a previous state, river meandering has five. These five instabilities arise when multiple boundary conditions fall into place (Stølum, 1997). To summarize from the earlier discussion, in the sandpile, (i) Grain-locking (friction) forces vertical build-up, (ii) rolling of surface grains at the angle of repose occurs, (iii) rupture of the stacked domains near the surface, and (iv) subsequent local sliding occurs. In a meandering system, (i) turbulence instability causes flow structures that lead to asymmetry in channel cross-sections in straight reaches, (ii) the asymmetry then produces a feedback, (iii) the subsequent flow instability causes lateral erosion, (iv) closed loop instabilities cause meanders to be cut off, and (v) neck instability causes deterioration of neck shape after cut-off (Stølum, 1997).

The opposing processes of sinuosity self-organize into a steady-state around a mean value of the sinuosity of a circle and are revealed through computer river simulations (Stølum, 1996). Stølum (1996) found through simulations that the dynamical state of SOC occurs when cut-offs act to destroy order while the river is in the ordered state, whereas in the chaotic state of high sinuosity, cut-offs act to maintain order by straightening the channel somewhat. Additionally, the presence of cut-offs acts to facilitate other local cut-offs through acceleration of local change, assisting in the development of spatiotemporal avalanches. These dynamics act to equalize the system around this critical state, fluctuating between chaos and order (Stølum, 1996). Further

examination is given to avalanche dynamics by Stølum, specifically to analyze fluctuations at the critical state, and make determinations of what components must be present for SOC to emerge. It has been concluded that in order for SOC to emerge, each of the opposing forces acts as an attractor for one of the forces and a repellent for the other, and that either force must repel different types of motion (Stølum, 1997).

Other recent work on the behavior of river meanders has examined them as trajectories in the phase space of sinuosity. Hooke (2003) described the range of behavior from accelerated active meandering to more stable meanders with lower rates or activity, and how they were categorized as exhibiting different trajectories when plotted in relation to rate and curvature. Through illustration in phase space, it can be determined that various types of behavior can be viewed as attractors of meandering systems. Whereas the conceptual model utilized in this research supports the oscillation between chaos and order in river meandering, the bigger aim is to recognize the phase space within each time series to build understanding of under what conditions different types of behavior occur (Hooke, 2003). SOC acknowledges that the response of the system is dependent on its state, and therefore, this research is a helpful coinciding perspective (Hooke, 2003).

Mountain Stream Characteristics

Mountain streams similar to those within the study area are unique due to their higher relief, generally steeper channel slopes, often reduced ability to meander, and consequently greater stream power. Gravel-bed streams are characterized by relatively featureless beds (Montgomery and Buffington, 1997). They differ from step-pool and pool-riffle channels because of their lack of tumbling flow and overall lower roughness

values. Additionally, these types of channels contain armored bed surfaces enabling a near-bankfull threshold for mobility (Montgomery and Buffington, 1997). These bed surfaces also indicate that the streams have a transport capacity greater than sediment supply, whereas other unarmored streams may have a more balanced state between transport capacity and sediment supply (Montgomery and Buffington, 1997).

In addition to gravel-bed streams, some portions within the study area are bedrock channels, meaning that they do not have a continuous alluvial bed. They are characterized by higher channel-boundary resistance and roughness from the bedrock along the channel (Wohl, 2000). They are usually confined between valley walls and have steeper channels than alluvial channels with the same drainage area (Montgomery and Buffington, 1997).

Fluvial Wood Impacts on Mountain Streams

Forced morphology such as the presence of fluvial wood can have significant impacts in mountain streams. Montgomery *et al.* (2003) recognize three themes that dominate the geomorphic research on the presence of wood in streams across scales: sediment routing, channel dynamics, and adjustment. For the purposes of this study, however, we are interested in the effects of present fluvial wood found within the channel at a steady time scale.

Mechanisms of fluvial wood such as sediment barriers cause deposition, usually upstream, creating a decrease in channel slope and an overall impediment to downstream movement of particles causing a highly variable sediment supply (Haschenburger and Rice, 2004). Faustini and Jones (2003) examine the effects of large woody debris in mountain boulder-rich streams in the western Cascades, Oregon. These streams are

similar to parts of those within the Upper Animas tributaries. They conclude that the effects of fluvial wood play an integral role in areas with large boulders in helping to create alluvial reaches in steep reaches in areas otherwise presumed to be composed of bedrock channels. In addition, Faustini and Jones (2003) find that courser bed load and large boulders increase the sediment-wood interaction through greater stability for wood accumulation.

Fluvial wood can act to create erosion, flow divergence, and the most common effect; sediment storage creating steps and pools in mountain drainage basins (Montgomery and Buffington, 1997). Fluvial wood in Rocky Mountain streams have been shown as functioning to create pools in the majority of cases (Richmond and Fausch, 1995). Wood obstructions cause water to scour pools, and depending on the type of obstruction from vertical to step, different types of pools are created (Montgomery *et al.*, 2003).

The fluvial wood found within small to medium mountain channels largely accumulates as debris dams that are perpendicular to the channel, and often cover its entire length (Piégay and Gurnell, 1997). Wood may remain stationary or be transported downstream depending on its size, and the size of the channel. Stable wood acts as an impediment to local flow hydraulics as well as an obstruction to sediment transport further obstructing the flow within the channel (Montgomery and Piégay, 2002).

There is not an abundance of research investigating the effects of large woody debris on bank stability in mountain rivers; however, Angradi and Schweiger (2004) inventoried over 6,000 pieces of large woody debris within the upper reaches of the Missouri river in North Dakota in order to examine the spatial variation of large woody

debris and shoreline type. They found that the highest densities of fluvial wood were found in areas along alluvial sand/silt shorelines, over 5,000 pieces and the fewest were found in areas armored with colluvium or bedrock, 388 pieces, with only slightly more in gravel-bed channels. They also concluded that fluvial wood was present four to five times more in forested areas than open land (Angradi and Schweiger, 2004). The results indicate that in rivers such as those within the study area, colluvium or bedrock gravel rivers, the least amount of wood is present. However, circumstances may be different in mountain stream where greater flow depth and large boulders may act to inhibit the downward motion of fluvial wood (Faustini and Jones, 2003).

Field Estimation Techniques

Fonstad and Marcus (2003) examine the presence of SOC in river systems through the measurement and context of bank erosion and mass wasting (failure), contending that it may be perceived as having spatial and temporal trends that exhibit power laws. Their research includes field data measured in three watersheds with relatively few human impacts on their morphology. They measured bank failure along increments of these streams, and plotted the magnitude and frequency of their occurrence. Their results support their simulations within CA, as power law distributions of the magnitude and frequency of bank failure were apparent (Fonstad and Marcus, 2003). In addition, the power-law slope gradient of each watershed coincides with overall channel slope, suggesting that channel slope is the primary factor influencing the strength of the power-law relationship (Fonstad and Marcus, 2003). More recently, Griffiths (2005) conducted a study based on the findings of Fonstad and Marcus (2003) in order to determine if similar results occur when utilizing similar field methods on three Welsh

rivers. Griffiths (2005) did, in fact, uncover strong power laws in the frequency-magnitude plots for all three of the rivers within the study area.

Summation

Previous research on the theories underlying power laws in nature provides a strong basis for further exploration into the existence and profusion of spectral and fractal patterns in geomorphic systems. SOC has proven to be a captivating explanation for power laws in river meanders and subsequent erosion, however, little research has been done to determine if these power laws exist in different types of rivers or if their occurrence is affected by the presence of fluvial wood and vegetation. This research will utilize and expand upon the field measurement techniques of Fonstad and Marcus (2003) in an attempt to further provide evidence of SOC in river systems. If successful, this research will testify to either the resilience or limitations of power laws in riverbank failure. Overall, the research may help to reiterate the notion that local process controls in rivers do not, in fact, bear much consequence on overall watershed health.

CHAPTER III

STUDY AREA

The study area for this research is the San Juan Mountains region of southwest Colorado, within the Upper Animas River watershed. Specifically, the study areas are the two tributaries that join the Animas River in the small old mining town of Silverton, Colorado: Mineral Creek and Cement Creek. The greater interest in these streams is significant due to the degradation of their water quality by the history of mining in the region. The mines have since been shut down, the primary income for the town is now tourism, yet the effects of historical mining in the region continue to fuel researchers and major rehabilitative efforts within the area (Robinson, 2000). It provides, therefore, a welcoming location for any type of research on the watershed, as well as a significant amount of data and existing research.

The Upper Animas watershed begins at elevations of over 4000 meters and ends at elevations of approximately 2800 meters in Silverton, Colorado. The approximate slope of Cement Creek is 0.032 whereas Mineral Creek has an approximate slope of 0.028. The climate varies significantly according to the elevation in the region; however, within the Upper Animas watershed, an average of 100-130 centimeters of precipitation is received, usually occurring in July and August as well as January through March. The average temperature ranges from 23° Celsius in July to -18° Celsius in January (Table 1).

Figure 3 is a location map of the Upper Animas Watershed region provided by the USGS Abandoned Mine Lands Initiative. It exhibits the peak elevations in the area as well as the main tributaries leading to the Animas River including Cement and Mineral Creeks.

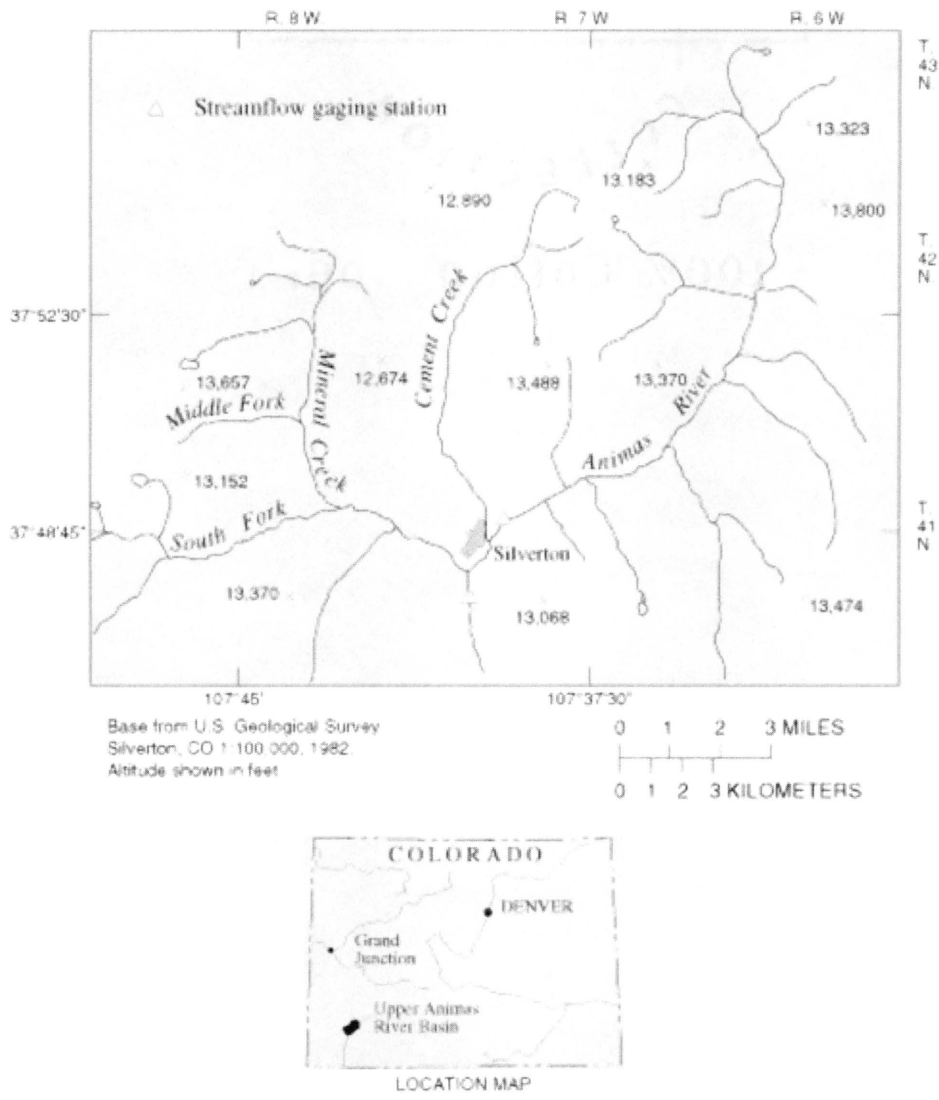


Figure 3. Location Map of the Upper Animas Watershed (USGS Abandoned Mine Lands Initiative 1998).

Watershed Characteristics	Upper Animas Watershed, CO
Drainage Area (km ²)	388
Precipitation (cm/yr)	100-130
Elevation (m)	2804-4206
General Geology	Intercaldera Lavas (hydrothermally altered)

Table 1. Upper Animas Watershed Characteristics (USGS Abandoned Mine Lands Initiative 1998)

The geologic make up of the Animas watershed is complex, with parent materials dating from the Precambrian era to recent alluvial deposits (McGarigal *et al.*, 2001). The study area is encompassed by the western part of the mid-late Tertiary age San Juan volcanic field, and is comprised of volcanic lava and rock from the San Juan Caldera and the Silverton Caldera (Lipman *et al.*, 1976). Other geologic activity has evolved from uplifts and then subsequent down-cutting that have allowed for the formation of the Animas and its tributaries with varying degrees of sediment deposition (Dalton *et al.*, 1999). Paleozoic and Mesozoic sedimentary rocks make up a significant portion of the general geology as shown in Figure 4. The geologic substrate of the Animas watershed is comprised of both extrusive and intrusive igneous rocks that have lead to a history of precious metal mining in the region.

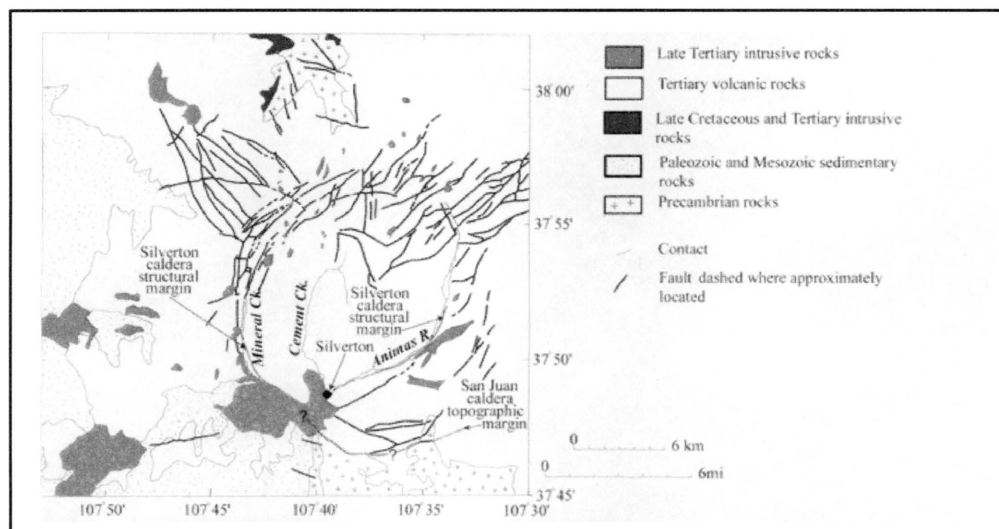


Figure 4. General Geology of Upper Animas Watershed (USGS Abandoned Mine Lands Initiative 1998).

The Animas watershed is currently under pressure from recreational activity and potential development. Therefore, a preliminary study on the dynamics of creeks within the watershed is warranted. Figure 5 illustrates the lowest reaches of the Mineral and Cement Creeks as they converge with the Upper Animas in Silverton. The relatively narrow channel widths and where it is situated near Silverton make the Upper Animas watershed logistically sound. In addition, it has an abundance of existing data due to research interests largely within the scope of monitoring the impacts of historical mining within the area. Accessibility limitations exist, however, in some small portions of the creeks because of steep slopes, unavailability of roads, and ice formations covering the rivers.



Figure 5. Location of Silverton, CO and Streams of Interest (Western Mapping Center, 1998).

CHAPTER IV

METHODOLOGY

Introduction

The goal of this field data collection is to inventory the quantity of bank failure along the entire stream lengths of Mineral and Cement Creeks within the Upper Animas Watershed, in order to determine the instability of the riverbanks. Next, the data are analyzed for the presence or absence of power laws within the study area. The purpose of this methodology seeks to answer the following questions:

- a. Do the magnitude and frequency of riverbank failure obey a power law?
- b. Is there a correlation between the slope of the power law with effective wood in and around the fluvial system?

Data Collection

The method of data collection roughly follows those utilized by Fonstad and Marcus (2003), with some minor modifications. For each of the two tributaries, measurements of observed bank failure are taken starting at the furthest upstream confluence. Waypoints are created within a GPS at each beginning and end of a 100 meter reach, and successive consecutive reaches are measured off while moving downstream through visual estimation with a laser range finder. Figure 6 displays the

endpoints of each reach for both creeks, overlaid onto a 1:250000 USGS topographic map.

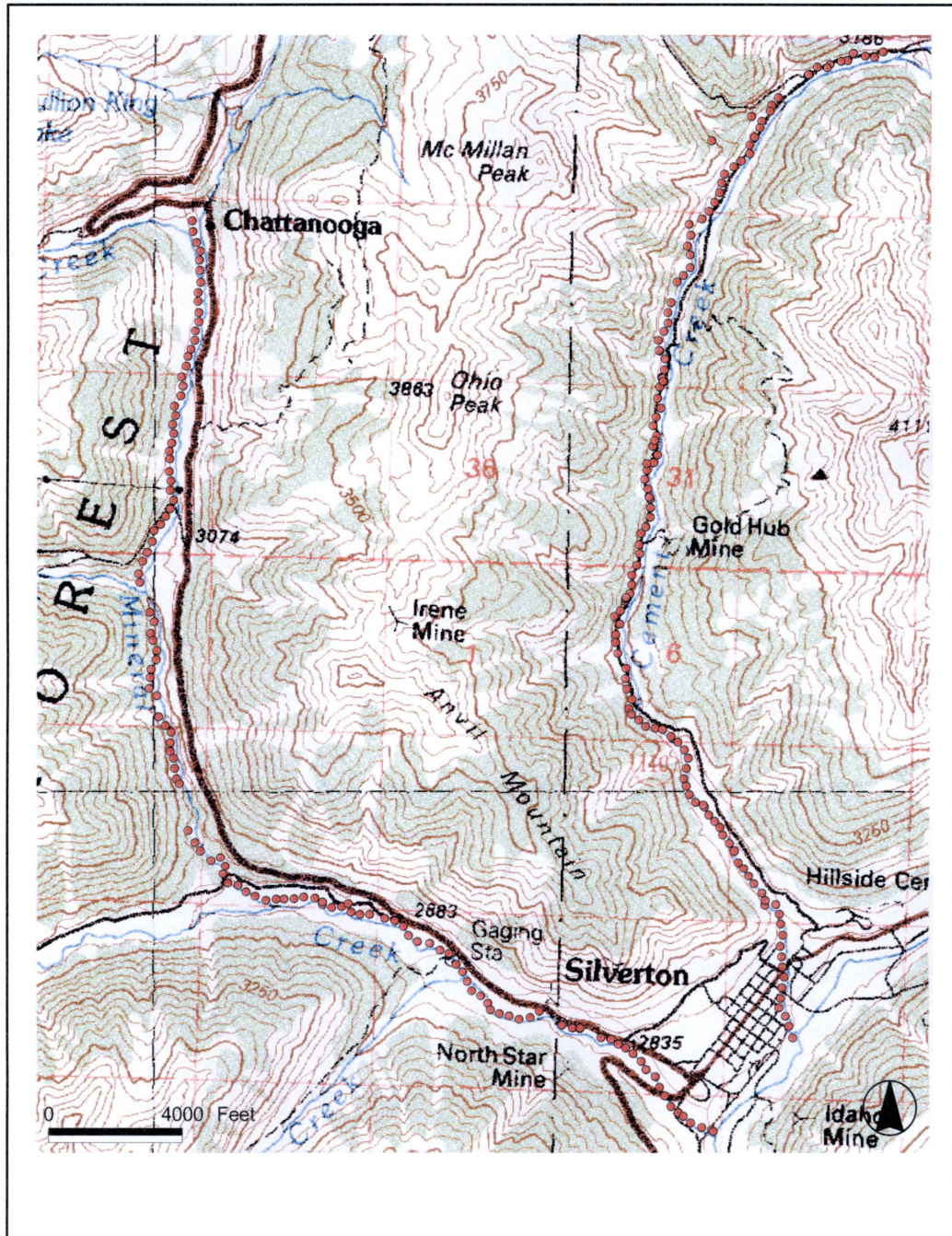


Figure 6. Location of Waypoints Bordering Each Reach in Study Area (USGS 1:250000 Topographic Map).

The interpretation of bank failure is subjective, therefore, characteristics developed by Fonstad and Marcus (2003) serve as guidelines for observation. These characteristics include the presence of recent failure scarps with minimal or no vegetation, undercutting in the bank walls, and any collapse of streamside biota into the channel (Fonstad and Marcus, 2003). Methods for measurement combine a visual estimation technique to determine the distance of the failure along each reach as well as a photogrammetry method.

A photogrammetric method utilizing a digital camera provides an alternative method for measuring bank failure along the reaches. This method is beneficial as it allows the analyst to frame the view of the channel to illustrate the active stream, the banks, and the vegetation (Graf and Randall, 1998). In addition, it also catalogs any fluvial wood that is present in areas of bank failure.

For every area of bank failure, one or more digital photos is taken with something or someone serving as the focal point, or the center of the photograph. Later, dimensions of the length of the bank failure are determined within AutoCAD, a computer drawing program. First, lines are delineated from the photo representing the areas to be measured; in this case the length of the bank failure, and then a tool within AutoCAD determines the coordinates, of the beginning and end point of the line (Figure 7). With these coordinates simple subtraction reveals the length of the line and hence the length of bank failure (Graf and Randall, 1998).

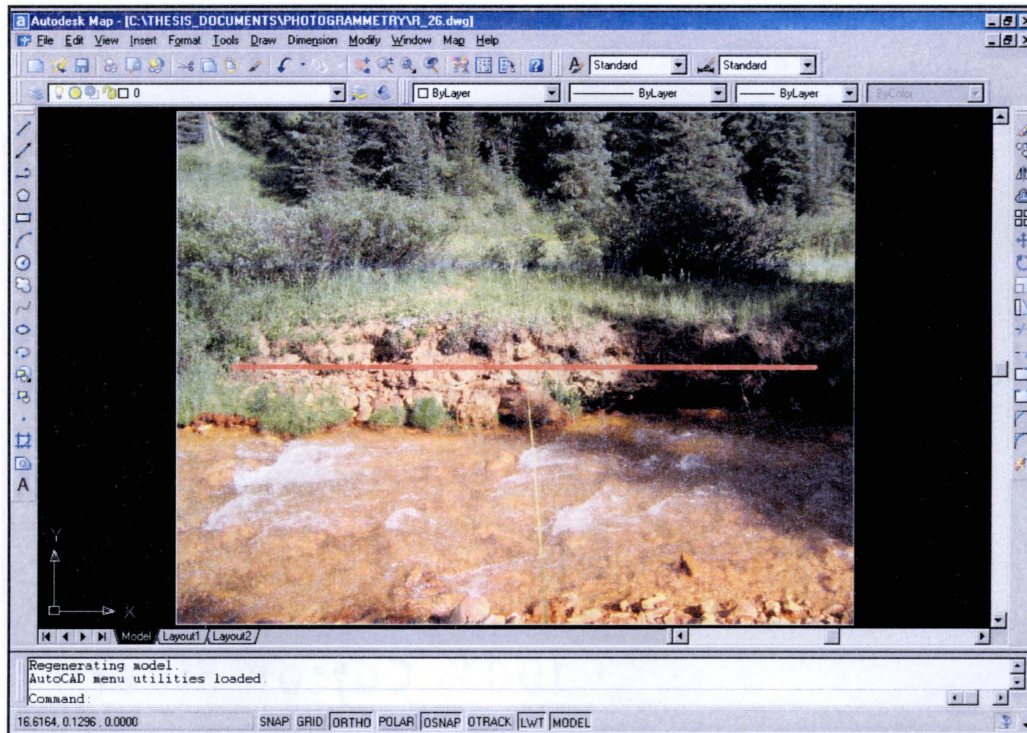


Figure 7. Delineated line showing the extent of the bank failure within a Photograph in AutoCad. Coordinates from each end are subtracted, giving a length of the line within the photo.

In addition, the depression angle and distance to principal point are determined in order to have all of the necessary variables for photogrammetric distance calculation. The ultimate goal of obtaining the depression angle is to determine the true horizon later from the photograph. The reason for this is that the true horizon is often difficult to determine in the field in riparian, or in this case, mountainous areas (Graf and Randall, 1998). Therefore, by measuring the tilt of the camera downward from the true horizon with a Brunton Compass, the depression angle is determined for later calculations. The distance to principal point is measured with a measuring tape. Figure 8 demonstrates the focal point of a photograph and a measuring tape extended from the focal point to the photographer. In this instance, the focal point is a small twig on top of the bank.



Figure 8. Example of Distance to Focal Point Determination. In this instance, the small twig on top of the bank is the focal point, or center of the photograph. The measuring tape is extended between the focal point and the photographer to obtain the necessary distance for length calculation.

Data Analysis

The following equation measures the length of bank failure with the photogrammetric method:

$$L = (d H) / (|ta| |\cos \Theta|)$$

where **L** = actual line length in meters, **d** = length of line in image in meters, **H** = height of camera above principal point in meters, **ta** is the measurement made from the image

from the x-axis to the line in the image in meters, and Θ is the depression angle (Graf and Randall, 1998).

Next, the equations are organized into columns into Excel for simple calculation with the already existing field measurements for each occurrence of bank failure. The data are organized in Excel and the percentage of failure for each 100 meter reach is calculated for the left and right banks. Next, the percentages are organized into classes based on amount of failure. The first class contains reaches with zero to five meters of failure, the second with six to fifteen meters, and so on until the largest class of failure, which is 45 to 55 meters.

The magnitude classes of bank failures for each 100m reach are plotted against the number of occurrences of bank failures of that size for each tributary by creating a log graph within Excel. This allows for direct comparisons of the resulting graphs for each basin.

The areas of high and low fluvial wood are estimated through ground photo interpretation. Large, or fluvial, wood is considered to encompass logs, limbs, and accumulation of debris within the stream or still attached to, yet fallen from, the banks. All fluvial wood with a diameter of 0.5 meters or greater and/or with a length of 0.5 meters in length is considered. Dalström and Nilsson (2004) use these measurements as qualifiers to determine large woody debris in old forest growths in Sweden. It is believed that this measurement size includes all wood of significant proportion. Figure 9 illustrates fluvial wood encountered within Mineral Creek. As shown in the photograph, there is wood wider and longer than 0.5 meters; enough to affect the morphology of the channel.

All of the photographs taken in the areas containing bank failure are evaluated for presence or absence of large wood of this description within the banks of the channel. The variability in the instability can be measured by comparing the slopes of the SOC power laws in areas of high wood versus those areas with low fluvial wood abundance.



Figure 9. Fluvial Wood in Channel of Mineral Creek.

CHAPTER V

RESULTS

Introduction

Data collected in the field provide a dataset intended for exploration into the spatial dynamics and potential existence of self-organized criticality within these mountain streams. The methods for field data collection are simplified to obtain data for areas only containing bank failure for rapid progression. Once the data are organized into spreadsheets, statistical analysis reveals a variety of results. In addition, spatial analysis displayed through maps offers a visual understanding of bank failure within the study area.

The findings from the data analysis strongly support the notion of SOC in riverbank erosion. This is due to the existence of power laws in almost every circumstance within the study area. In addition, the presence of fluvial wood in areas of bank failure may result in greater stabilization of the surrounding banks as evidenced by greater tau slope values.

Tables 2 and 3 display the magnitude and frequency results of the bank failure distributions within both creeks. It is easy to note that the largest number of bank failure sizes fall into the 0-5 meter bin, supporting the idea that smaller events in physical systems occur with more frequency.

Mineral Creek Right Bank		Mineral Creek Left Bank	
Magnitude Frequency	Magnitude Failure Size (m)	Magnitude Frequency	Magnitude Failure Size (m)
124	0-5	118	0-5
4	10-15	5	10-15
1	15-20	4	15-20
1	25-30	3	25-30
1	30-35	1	30-35

Table 2. Bins of Bank Failure Classes for Mineral Creek

Cement Creek Right Bank		Cement Creek Left Bank	
Magnitude Frequency	Magnitude Failure Size (m)	Magnitude Frequency	Magnitude Failure Size (m)
95	0-5	100	0-5
5	5-10	5	5-10
1	10-15	2	10-15
8	15-20	0	15-20
2	20-25	1	20-25
3	25-30	0	25-30

Table 3. Bins of Bank Failure Classes for Cement Creek

The Spatial Distribution of Bank Failures

The spatial distribution of bank failure within Cement and Mineral creeks is varied throughout the stream lengths, with the exception of the furthest downstream reaches, where minimal failure was detected. This minimal failure, although at first glance unusual, is due in some part to the various channelization and human-made developments that increase as the streams move towards their confluence at the Animas River within Silverton. Although a heterogeneous pattern of failures does exist throughout the stream lengths, the magnitude/frequency of these events obeys a power law structure in every instance studied. Figures 10-13 display the distribution of the bank failures for each of the creeks.

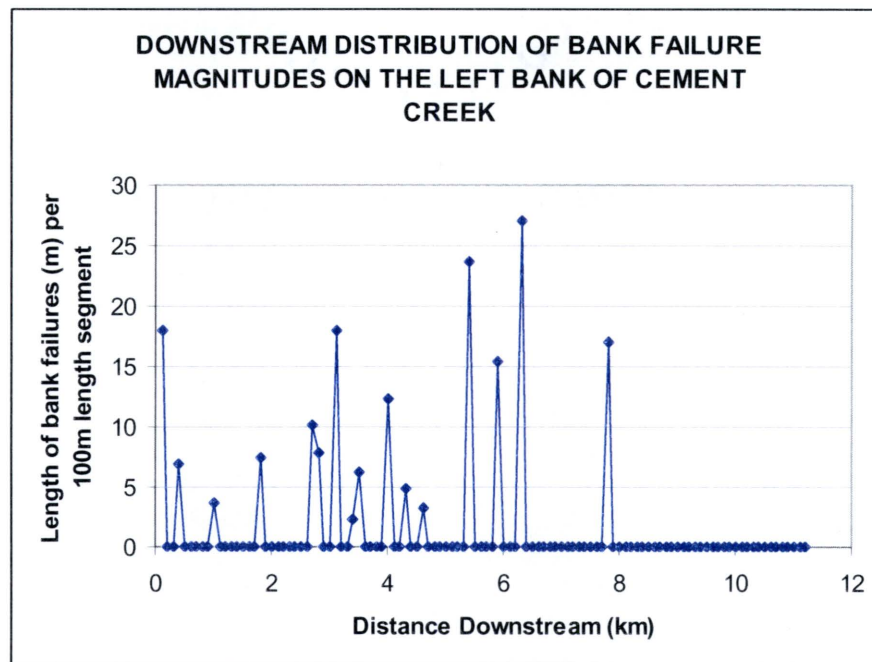


Figure 10. Left Bank Failure Downstream Distribution for Cement Creek.

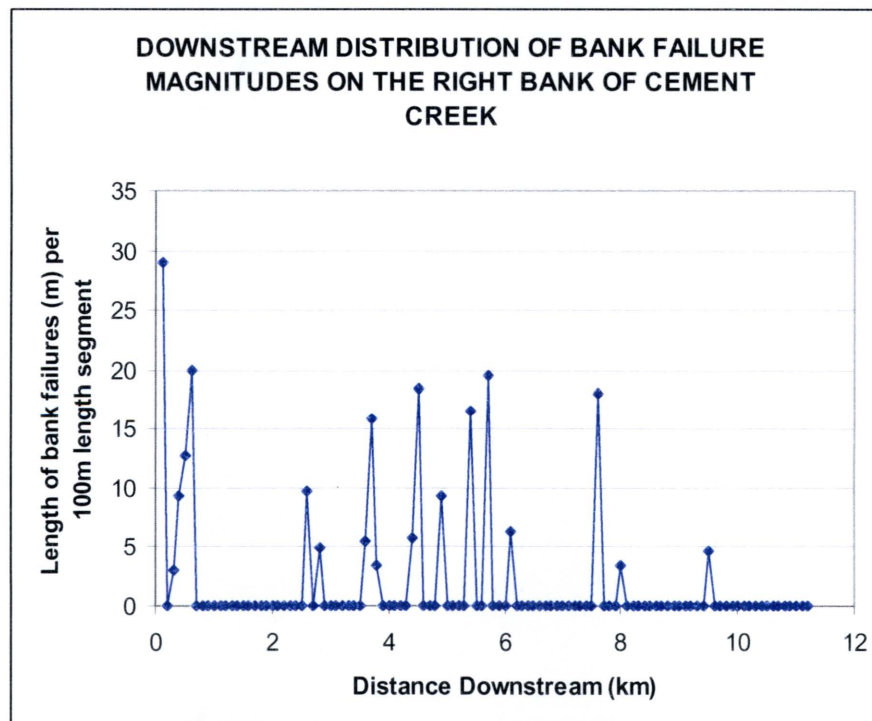


Figure 11. Right Bank Failure Downstream Distribution for Cement Creek.

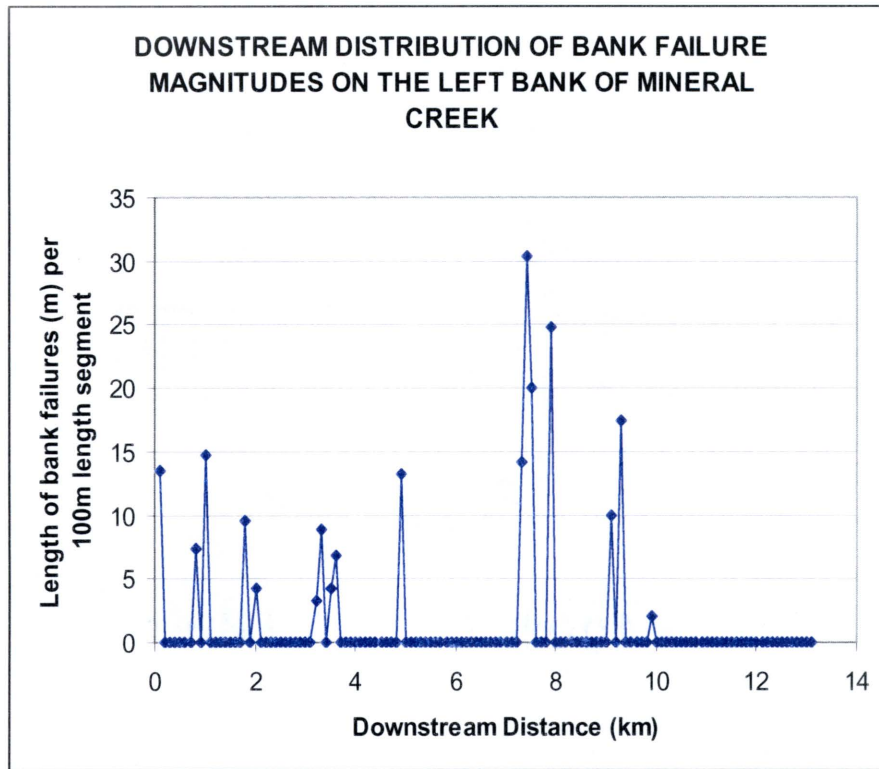


Figure 12. Left Bank Failure Downstream Distribution for Mineral Creek.

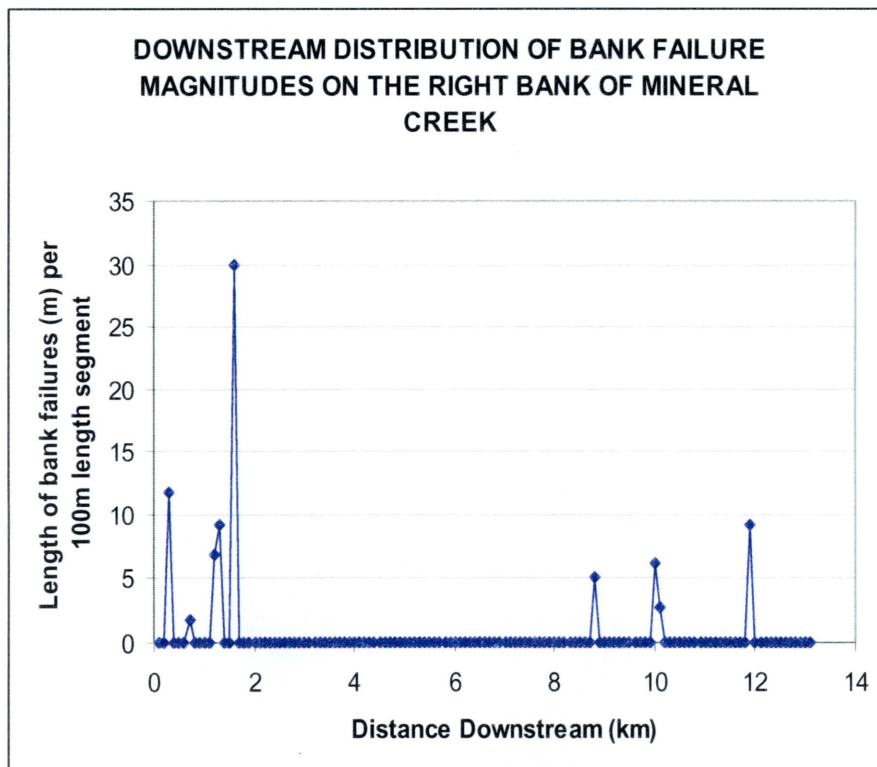


Figure 13. Right Bank Failure Downstream Distribution for Mineral Creek.

In order to provide a spatial perspective on the distribution of failure, GPS points taken in the field at the beginning of each new reach are first imported into ArcView. The accompanying database providing the locations are then joined with the bank failure as well as fluvial wood data in order to display spatial variations of failure. Figures 14 and 15 reveal the heterogeneous patterns of magnitude and frequency of occurrences for each reach. Despite these seemingly random patterns, significant power laws were detected unfolding a scaling pattern in line with SOC.

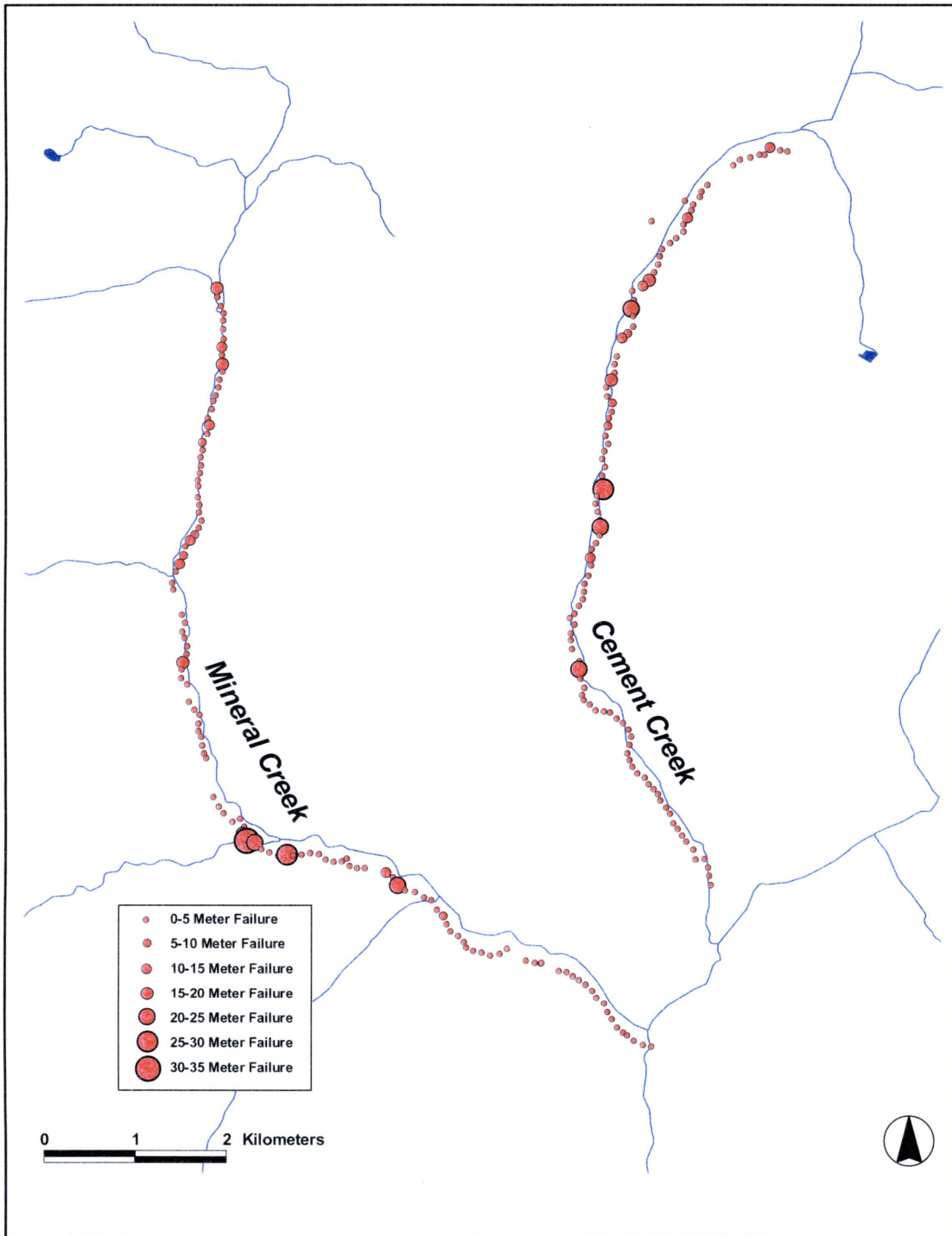


Figure 14. Locations of Left Bank Failure Distribution for Mineral and Cement Creeks.

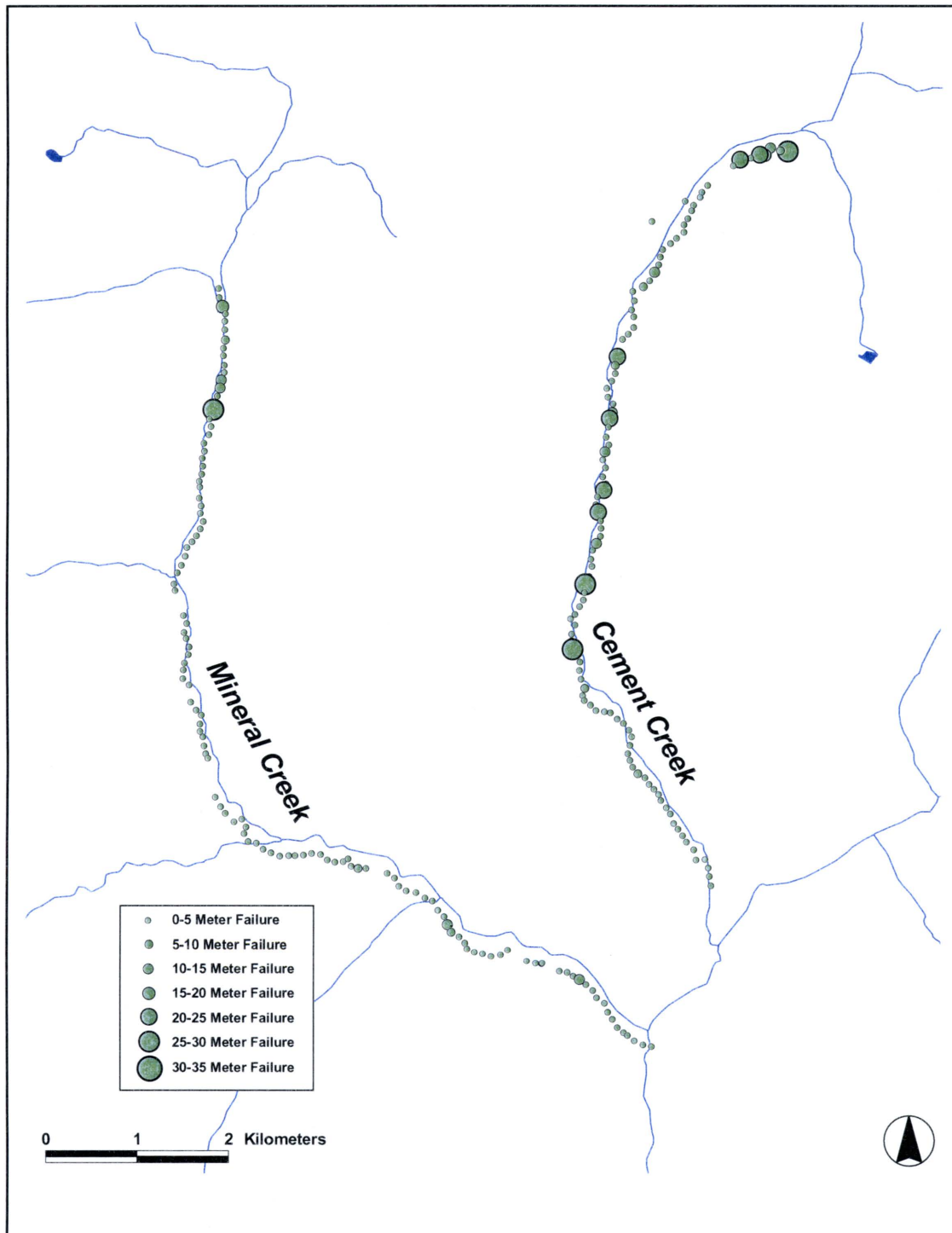


Figure 15. Locations of Right Bank Failure Distribution for Mineral and Cement Creeks.

The Magnitude and Frequency of Bank Failures

The results of the log graphs containing the magnitude and frequency of bank failure occurrence reveal varied, yet promising, results. The overall slope of the riverbank power laws within the two tributaries is 0.475, making these streams not as susceptible to small frequent sediment pulses (Table 4). The overall tau slope value for Cement and Mineral Creek is lower compared to those found in previous studies measuring bank failure, namely Fonstad and Marcus' (2003) research in Yellowstone Park and Griffiths' (2005) research in Wales. This demonstrates that the streams of the San Juan Mountains are more sensitive to major geomorphic shifts, or greater changes in the channel and surrounding landforms. Additionally, a slightly higher tau slope exists for Cement Creek than for Mineral Creek. This corresponds with the channel slopes of each creek, with that of the Cement being slightly steeper.

This may be due to the greater channel slopes of the study area. Increased stream energy allows for easier transmission of smaller events, which may inhibit build-up of sediment, fluvial wood, and other bank materials necessary for greater failures (Fonstad and Marcus, 2003). Because the tau slopes for the creeks are not very great, these materials may be accumulating towards a critical point that may lead to a large failure. Currently, no abundance of bank failure exists, and if the theory of SOC does indeed apply, a large event may occur at any point within the watersheds regardless of planning measures.

BASIN	BANK	TAU	R-SQUARED
CEMENT	LEFT	0.3827	0.7768
CEMENT	RIGHT	0.3498	0.4511
CEMENT	BOTH	0.4954	0.8076
CEMENT	LEFT WITH WOOD LEFT WITHOUT	0.6483	0.9998
CEMENT	WOOD	0.4968	0.4132
CEMENT	RIGHT WITH WOOD RIGHT WITHOUT	0.5747	0.4626
CEMENT	WOOD	0.7621	0.4323
CEMENT	BOTH WITH WOOD BOTH WITHOUT	0.5066	0.2195
CEMENT	WOOD	0.6743	0.3579
MINERAL	LEFT	0.3976	0.8599
MINERAL	RIGHT	0.3253	0.7870
MINERAL	BOTH	0.4541	0.8884
MINERAL	LEFT WITH WOOD LEFT WITHOUT	0.6817	0.2093
MINERAL	WOOD	0.8438	0.9259
MINERAL	RIGHT WITH WOOD RIGHT WITHOUT	1.5850	1.0000
MINERAL	WOOD	0.3730	0.8756
MINERAL	BOTH WITH WOOD BOTH WITHOUT	0.1064	0.0097
MINERAL	WOOD	0.8233	0.7427

Table 4. Power Law Statistics for Bank Failure Occurrences

Fluvial Wood and its Effects on Bank Failure Power Laws

Tables 5 and 6 below illustrate the results of the bins of bank failure frequency-magnitude for failure occurring in areas with fluvial wood present. When the tables are compared, it is also apparent that Cement Creek contains a much greater amount of fluvial wood in areas of bank failure than Mineral Creek. The r-squared percentages from Table 7 for fluvial wood within the creeks also supports the understanding that Mineral Creek in particular is lacking significant quantities of fluvial wood in the presence of bank failure to make any positive claim that they obey a power law.

Cement Creek Right Bank		Cement Creek Left Bank	
Magnitude Frequency	Magnitude Failure Size (m)	Magnitude Frequency	Magnitude Failure Size (m)
8	0-5	12	0-5
3	10-15	4	10-15
1	15-20	0	15-20
4	25-30	1	25-30
1	35-40	0	30-35

Table 5. Bins of Bank Failure Classes with Fluvial Wood for Cement Creek

Mineral Creek Right Bank		Mineral Creek Left Bank	
Magnitude Frequency	Magnitude Failure Size (m)	Magnitude Frequency	Magnitude Failure Size (m)
2	0-5	2	0-5
0	10-15	2	10-15
1	15-20	3	15-20
0	25-30	0	25-30
0	30-35	1	30-35

Table 6. Bins of Bank Failure Classes with Fluvial Wood for Mineral Creek

Two out of four slopes measured for reaches containing fluvial wood within the study area contain a greater slope when compared to those reaches without fluvial wood. This indicates that the presence of fluvial wood within the stream bed may act to stabilize the riverbanks. The other two slopes, conversely, would result in fluvial wood acting in an opposite fashion: destabilizing riverbanks. Insufficient data present within the two creeks exists to make predictions about the effects of fluvial wood on bank stability. However, the overall lower slopes of the banks measured without fluvial wood than those with fluvial wood support the notion in geomorphology that these areas are more susceptible to frequent large events and greater change.

BASIN	BANK	TAU	R-SQUARED
CEMENT	LEFT WITH WOOD	0.6483	0.9998
CEMENT	LEFT WITHOUT WOOD	0.4968	0.4132
CEMENT	RIGHT WITH WOOD	0.5747	0.4626
CEMENT	RIGHT WITHOUT WOOD	0.7621	0.4323
MINERAL	LEFT WITH WOOD	0.6817	0.2093
MINERAL	LEFT WITHOUT WOOD	0.8438	0.9259
MINERAL	RIGHT WITH WOOD	1.5850	1.0000
MINERAL	RIGHT WITHOUT WOOD	0.3730	0.8756

Table 7. Comparison of Tau Slopes for Bank Failure With and Without Fluvial Wood

The scatter plots in Figures 16 and 17 for areas of bank failure with and without fluvial wood within the two creeks reveal the uncertainties due to lack of data within the study area. Areas of bank failure with fluvial wood within the creeks are not frequent enough to extrapolate conclusions regarding the effects that fluvial wood have on the power law structure of this study area.

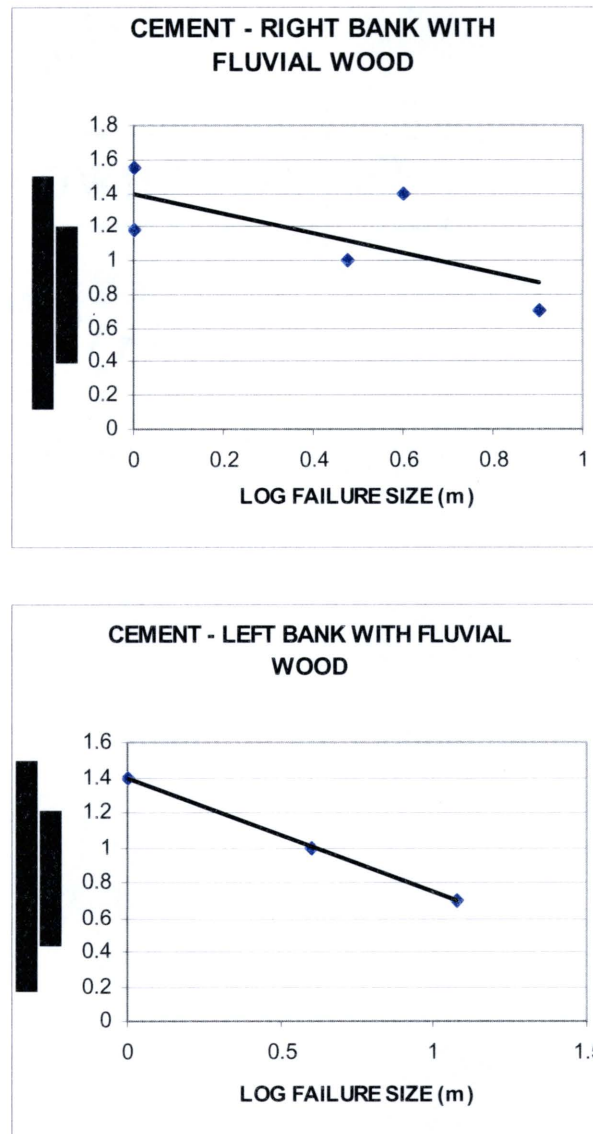


Figure 16. Power Law Distributions of Presence of Fluvial Wood in Cement Creek.

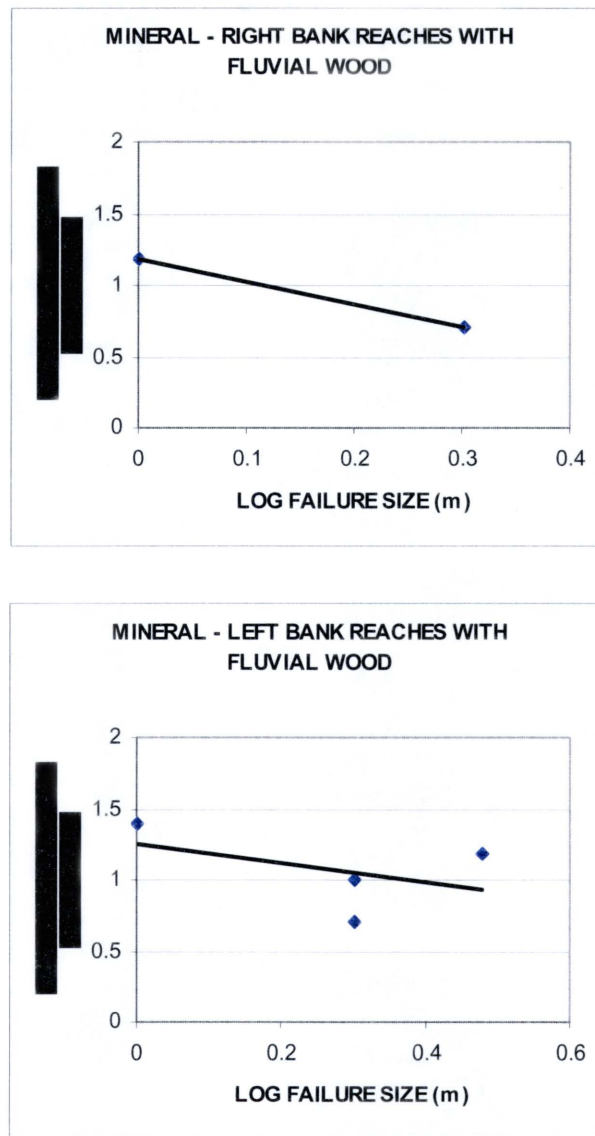


Figure 17. Power Law Distributions of Presence of Fluvial Wood in Mineral Creek.

CHAPTER VI

DISCUSSION AND CONCLUSION

Discussion

Methodology

The methods of data collection in the field are successful; nevertheless, improvements may be made based on some of the realities discovered when hiking along mountain streams. Initially, there are limitations on the study area because of the rivers' locations nestled in between extraordinarily steep slopes of the mountains in some of the higher elevations. Accessibility to these sections of the rivers is extremely difficult at best. Therefore, the Upper Animas River was left out all together from the study area. Future researchers may consider developing a method for encompassing these inaccessible areas remotely, in order to collect data from all of the streams for a more holistic study.

The photogrammetry method is beneficial in that it provides visual evidence of the present bank failure; however, it requires a very carefully positioned photographer, something that is not always possible. When interpreting the failure lengths from the photographs it is only accurate when the photograph is perfectly centered. Unfortunately, this is not the case for many of the photographs because of the riparian obstructions and

very steep bank slopes impeding the photographer, and in the end, simple measurements using a tape measure are adequate.

Furthermore, photographs are available only for areas with bank failure, and therefore, evidence of fluvial wood is only determined in these locations. This limits the analysis possible for the study site, as it would be significant to have an account of all areas with wood within each reach, and not confined to areas of erosion. Therefore, future research warrants an enhanced method of data collection regarding additional river characteristics.

Results

The existence of power laws in the magnitude and frequency of bank failure events in this mountain river system allow it to remain in a critical state. This indicates that the entire basin is acting as a whole functioning unit that may no longer be characterized through isolated contingent events (Bak and Paczuski, 1996). Although some power laws are stronger than others, it is remarkable that with even a limited dataset they are detected in almost every situation.

Overall, there is not an abundance of bank failure within the two streams. This may be due to the confined nature of the creeks within areas where it is bound by steep narrow slopes. This inhibits the creeks ability to meander and erode. Furthermore, a large portion of the creeks have bedrock channel beds that also act to stabilize the system.

Another factor that may be contributing to the results, however, is the channelization and other human-made alterations to the streams as they weave through the town of Silverton. No bank erosion is detected in these areas and it is influenced by

these circumstances while previous studies, for example, were conducted within watersheds that were not directly impacted by development, such as in national parks.

When analyzing tau slopes, the lower its value, the higher the proportions of failures are greater in magnitude. The results of the Fonstad and Marcus (2003) study have an overall tau slope range of 1.070-1.492 for the three basins in Yellowstone. The results of Griffiths (2005) study had an overall tau slope range of 0.9187- 1.7865 for the three basins in Wales. The results of this study have a range of tau slopes from 0.3253-0.4954 for the two basins in Silverton, Colorado. Therefore, out of the three existing field studies testing power laws in riverbank failure, Mineral and Cement Creeks have the lowest tau values and consequently are more susceptible to major geomorphic shifts.

These lower tau slopes for this area are surprising. In the past, it has been theorized that the greater the channel slope, the greater the tau slope in most cases (Fonstad and Marcus, 2003). This study area is unique in that it does have greater channel slopes and less meandering, which at first thought would act to inhibit greater bank failures. Because the power law slopes are low, the watersheds are not as susceptible to smaller, more frequent, sediment pulses.

One possible reason behind this shift in results may be that because there is not a large floodplain, the rivers are unable to meander, and therefore energy dissipates through other outlets such as rapids. Another possibility for this anomaly is that the streams are unable to transmit energy as readily because of steeper hillslopes. In addition, significant areas of braiding occur on the valley floors that may act to slow down the stream-power. Channels frequently change course in these areas during rain events.

An observation of the effects that natural impacts may have on watershed organization is also accomplished through the division of this power law into rich and poor fluvial wood segments. This allows for the interpretation of the direct interactions between organic and geomorphic processes and how they may influence SOC and river systems. Fluvial instability is the result of many factors such as gross channel morphology, stream power, riverbank material, and grain-level processes, and fluvial wood can control some amount of bank instability and sediment supply to rivers. The results are promising within the study, yet data are limited, and further study is warranted in order to gain more confidence in these impacts.

Implications

A successful determination of power laws within the scope of this study adds a significant addition to the theory of SOC in bank failure. Implications are widespread in terms of stream management and restoration. Traditionally, stream management is determined through analysis of local cross-sections that determine the hydraulic geometry of the stream and other physical parameters, with the underlying assumption that changes are due to extreme events or else are an effect of these local basin characteristics. This assumption leads to the practice of structural alterations within the basin, assuming that a stable reach may be achieved if all of the natural physical parameters are upheld. If the theory of SOC indeed applies to bank failure, then this type of management is problematic as a long-term solution.

Because SOC implies that the entire system is maintaining itself at a critical state, local erosion events will vary as a component of a basin-wide distribution of bank failure and is not contingent upon the local characteristics of the stream (Fonstad and Marcus,

2003). It is only through observation of the distribution of all of the failures within the river systems that it is possible to achieve an understanding of what state the watershed is acting to predict long-term, system-wide, events (Fonstad and Marcus, 2003).

Future Research Possibilities

Further research for this study area may include the development of a spatial model simulating the effects of water flow, sedimentation, and erosion with a channel. SOC is an exciting theory to test using computational simulation of river systems since the new generation of 2 and 3-dimensional models, specifically CA. The melding of observational and theoretical methodologies has been a successful strategy for evaluating SOC in river systems, although the development of dynamical models to test SOC has only really begun to be explored in the last ten years.

CA is a method of simulation that has been employed by geographers due to its inherently spatial properties as it reveals movement over space and has been utilized successfully in river studies (Murray *et al.*, 1994; Murray and Paola, 1997; Thomas and Nicholas, 2002; Murray and Paola, 2003; Fonstad and Marcus, 2003). In addition to the construction of a basic model of riverbank behavior, vegetation rules may be added in order to determine if rules regarding the behavior of fluvial wood act to stabilize the channel. Modeling may provide a second source of evidence for SOC in river systems and reveal river dynamics over a longer period of time for they are not limited to present-day observations.

Other future research may involve a similar field study with more data collection such as discharge, local channel slope, and a full inventory of fluvial wood as well as

riparian areas along the banks. This would allow for better correlative studies between the effects of these local characteristics with the overall power law slopes in the streams.

Conclusion

This study attempts to answer the questions, “Can the presence of SOC be determined in the bank failure of a mountain river system?” and “Does the presence or absence of fluvial wood affect these theorized power laws?” To accomplish this goal, field work was undertaken within two mountain creeks within the Upper Animas basin in Silverton, CO, measuring the length of bank failure along 100m reaches and subsequently plotted to determine the magnitude and frequency of the failure within each basin.

The results of this research support the claim that bank failure is part of an SOC system. Power law distributions prevailed for the magnitude and frequency of bank failure within the complete stream lengths of Cement and Mineral Creeks. These distributions are necessary in order for the river systems to maintain a critical state.

Overall, SOC continues to be an intriguing answer to the mysteries of power laws in nature and the more research that is done on the subject of its presence within geomorphology generally and river systems specifically, the more we may understand the underlying order within physical systems, leading to better management practices.

APPENDIX I

CEMENT CREEK BANK FAILURE DATA

The data represented in Appendix I displays the bank failure in Cement Creek. The abbreviations for the data fields are as follows: FAIL LENGTH is the length of bank failure in meters, SIDE is the left or right bank where it occurs, FRAME # is the frame number in the camera, DEPRESS is the depression angle of the camera, ID is the number of the photo when there are more than one for a single stretch of failure, LINE is the length in meters between the camera and the principal point, and PRINCIPAL POINT is the center point of the photograph.

Cement Creek – Reach Number 1, Failure 1

View of Right Bank from Left Bank

FAIL LENGTH (m)	SIDE	FRAME #	DEPPRESS	ID	LINE	PRINCIPAL POINT
18	L	74	170		17	ORANGE ROCK

Cement Creek – Reach 1, Failure 2



Photo i.

FAIL LENGTH (m)	SIDE	FRAME #	DEPPRESS	ID	LINE	PRINCIPAL POINT
29	R	1	178	i	6	ORANGE ROCK
		2	178	ii	4.7	ORANGE ROCK
		3	178	iii	4.8	ORANGE ROCK
		4	178	iv	4.32	ORANGE ROCK



Photo ii.

FAIL LENGTH (m)	SIDE	FRAME #	DEPPRESS	ID	LINE	PRINCIPAL POINT
29	R	1	178	i	6	ORANGE ROCK
		2	178	ii	4.7	ORANGE ROCK
		3	178	iii	4.8	ORANGE ROCK
		4	178	iv	4.32	ORANGE ROCK



Photo iii.

FAIL LENGTH (m)	SIDE	FRAME #	DEPPRESS	ID	LINE	PRINCIPAL POINT
29	R	1	178	i	6	ORANGE ROCK
		2	178	ii	4.7	ORANGE ROCK
		3	178	iii	4.8	ORANGE ROCK
		4	178	iv	4.32	ORANGE ROCK



Photo iv.

FAIL LENGTH (m)	SIDE	FRAME #	DEPPRESS	ID	LINE	PRINCIPAL POINT
29	R	1	178	i	6	ORANGE ROCK
		2	178	ii	4.7	ORANGE ROCK
		3	178	iii	4.8	ORANGE ROCK
		4	178	iv	4.32	ORANGE ROCK

Cement Creek – Reach Number 2, Failure 1



View of Right Bank from Left Bank.

FAIL LENGTH (m)	SIDE	FRAME #	DEPPRESS	ID	LINE	PRINCIPAL POINT
11.8	R	6	142		7.2	ORANGE ROCK

Cement Creek – Reach Number 2, Failure 2



Photo i.

FAIL LENGTH (m)	SIDE	FRAME #	DEPPRESS	ID	LINE	PRINCIPAL POINT
15.7	R	7	163	i	10.2	ORANGE ROCK
		8	165	ii	12.5	ORANGE ROCK



Photo ii.

FAIL LENGTH (m)	SIDE	FRAME #	DEPPRESS	ID	LINE	PRINCIPAL POINT
15.7	R	7	163	i	10.2	ORANGE ROCK
		8	165	ii	12.5	ORANGE ROCK

Cement Creek – Reach 3, Failure 1

View of Right Bank from Left Bank.

FAIL LENGTH (m)	SIDE	FRAME #	DEPPRESS	ID	LINE	PRINCIPAL POINT
3		9	185		5	ORANGE ROCK

Cement Creek – Reach 4, Failure 1

View of Right Bank from Left Bank.

FAIL LENGTH (m)	SIDE	FRAME #	DEPRESS	ID	LINE	PRINCIPAL POINT
6.9	L	11	145		7.6	ORANGE ROCK

Cement Creek – Reach 4, Failure 2



Photo i.

FAIL LENGTH (m)	SIDE	FRAME #	DEPPRESS	ID	LINE	PRINCIPAL POINT
9.3	R	12	170	i	8.2	ORANGE ROCK
		13	183	ii	7.6	ORANGE ROCK



Photo ii.

FAIL LENGTH (m)	SIDE	FRAME #	DEPPRESS	ID	LINE	PRINCIPAL POINT
9.3	R	12	170	i	8.2	ORANGE ROCK
		13	183	ii	7.6	ORANGE ROCK

Cement Creek – Reach 5, Failure 1



Photo i.

FAIL LENGTH (m)	SIDE	FRAME #	DEPPRESS	ID	LINE	PRINCIPAL POINT
12.7	R	14	165	i	8.6	RT. FLAG
		15	155	ii	4.6	ORANGE ROCK



Photo ii.

FAIL LENGTH (m)	SIDE	FRAME #	DEPPRESS	ID	LINE	PRINCIPAL POINT
12.7	R	14	165	i	8.6	RT. FLAG
		15	155	ii	4.6	ORANGE ROCK

Cement Creek – Reach 6, Failure 1

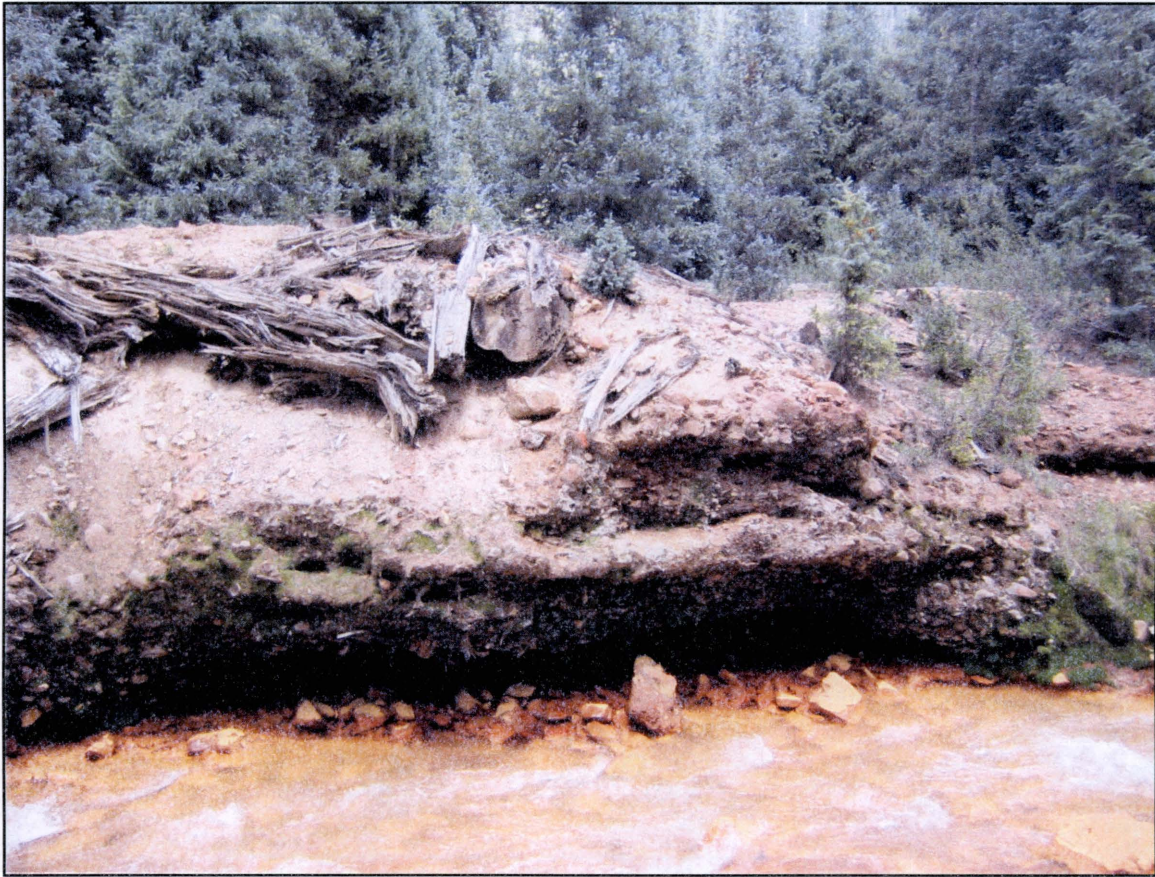


Photo i.

FAIL LENGTH (m)	SIDE	FRAME #	DEPPRESS	ID	LINE	PRINCIPAL POINT
		16	205	i	8.4	RIBBON ON WOOD
		17	160	ii	11.7	RIBBON ON WOOD



Photo ii.

FAIL LENGTH (m)	SIDE	FRAME #	DEPPRESS	ID	LINE	PRINCIPAL POINT
		16	205	i	8.4	RIBBON ON WOOD
		17	160	ii	11.7	RIBBON ON WOOD

Cement Creek – Reach 8, Failure 1



Photo i.

FAIL LENGTH (m)	SIDE	FRAME #	DEPRESS	ID	LINE	PRINCIPAL POINT
11.6	R	19	190	i	7.5	ORANGE ROCK
		20	148	ii	7.3	ORANGE ROCK

Cement Creek – Reach 8, Failure 1



Photo ii.

FAIL LENGTH (m)	SIDE	FRAME #	DEPPRESS	ID	LINE	PRINCIPAL POINT
11.6	R	19	190	i	7.5	ORANGE ROCK
		20	148	ii	7.3	ORANGE ROCK

Cement Creek – Reach 8, Failure 2



Photo i.

FAIL LENGTH (m)	SIDE	FRAME #	DEPPRESS	ID	LINE	PRINCIPAL POINT
5.3	R	21	185	i	7.8	ORANGE ROCK
		22	175	ii	7	ORANGE ROCK



Photo ii.

FAIL LENGTH (m)	SIDE	FRAME #	DEPPRESS	ID	LINE	PRINCIPAL POINT
5.3	R	21	185	i	7.8	ORANGE ROCK
		22	175	ii	7	ORANGE ROCK

Cement Creek – Reach 10, Failure 1

View of Left Bank from Right Bank.

FAIL LENGTH (m)	SIDE	FRAME #	DEPRESS	ID	LINE	PRINCIPAL POINT
3.7	L	23	210		6.5	ORANGE ROCK

Cement Creek – Reach 18, Failure 1

View of Left Bank from Right Bank.

FAIL LENGTH (m)	SIDE	FRAME #	DEPPRESS	ID	LINE	PRINCIPAL POINT
7.5	L	26	195		8	ORANGE ROCK

Cement Creek – Reach 26, Failure 1



View of Right Bank from Left Bank.

FAIL LENGTH (m)	SIDE	FRAME #	DEPPRESS	ID	LINE	PRINCIPAL POINT
9.7	R		340		12.8	MINDY

Cement Creek – Reach 27, Failure 1



View of Left Bank from Right Bank.

FAIL LENGTH (m)	SIDE	FRAME #	DEPPRESS	ID	LINE	PRINCIPAL POINT
10.2	L		210		13.6	MINDY

Cement Creek – Reach 28, Failure 1



View of Left Bank from Right Bank.

FAIL LENGTH (m)	SIDE	FRAME #	DEPRESS	ID	LINE	PRINCIPAL POINT
7.9	L		205		10	MINDY

Cement Creek – Reach 28, Failure 2

View of Right Bank from Left Bank.

FAIL LENGTH (m)	SIDE	FRAME #	DEPRESS	ID	LINE	PRINCIPAL POINT
4.9	R		210		5.3	BERNIE

Cement Creek – Reach 31, Failure 1



Photo i.

FAIL LENGTH (m)	SIDE	FRAME #	DEPRESS	ID	LINE	PRINCIPAL POINT
18	L		195	i	4.6	BERNIE
			200	ii	5.4	BERNIE
			170	iii	7.2	BERNIE



Photo ii.

FAIL LENGTH (m)	SIDE	FRAME #	DEPPRESS	ID	LINE	PRINCIPAL POINT
18	L		195	i	4.6	BERNIE
			200	ii	5.4	BERNIE
			170	iii	7.2	BERNIE



Photo iii.

FAIL LENGTH (m)	SIDE	FRAME #	DEPPRESS	ID	LINE	PRINCIPAL POINT
18	L		195	i	4.6	BERNIE
			200	ii	5.4	BERNIE
			170	iii	7.2	BERNIE

Cement Creek – Reach 34, Failure 1



View of Left Bank from Right Bank.

FAIL LENGTH (m)	SIDE	FRAME #	DEPPRESS	ID	LINE	PRINCIPAL POINT
2.3	L		195		9	MINDY

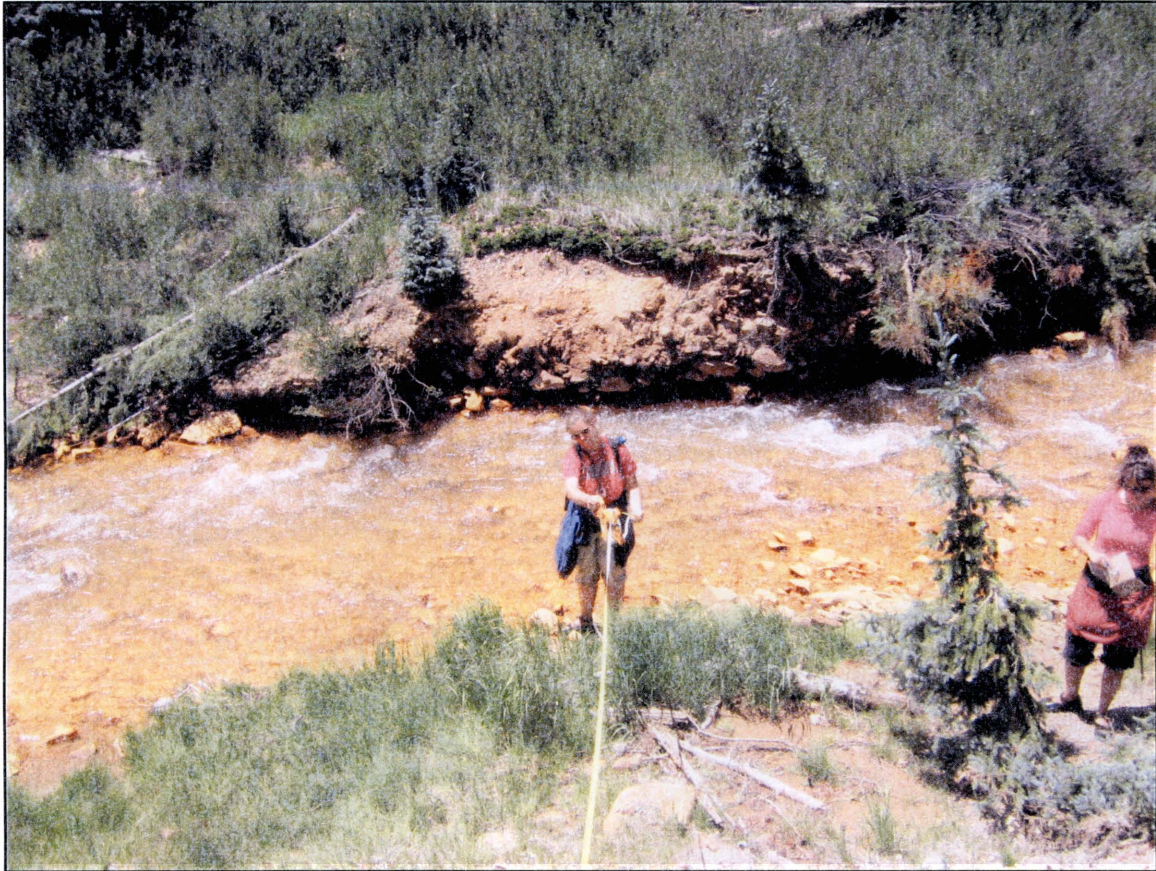
Cement Creek – Reach 35, Failure 1



View of Left Bank from Right Bank.

FAIL LENGTH (m)	SIDE	FRAME #	DEPPRESS	ID	LINE	PRINCIPAL POINT
6.2	L		175		9.2	BERNIE

Cement Creek – Reach 36, Failure 1



View of Right Bank from Left Bank

FAIL LENGTH (m)	SIDE	FRAME #	DEPPRESS	ID	LINE	PRINCIPAL POINT
5.5	R		310		7.8	MINDY

Cement Creek – Reach 37, Failure 1



View of Right Bank from Left Bank.

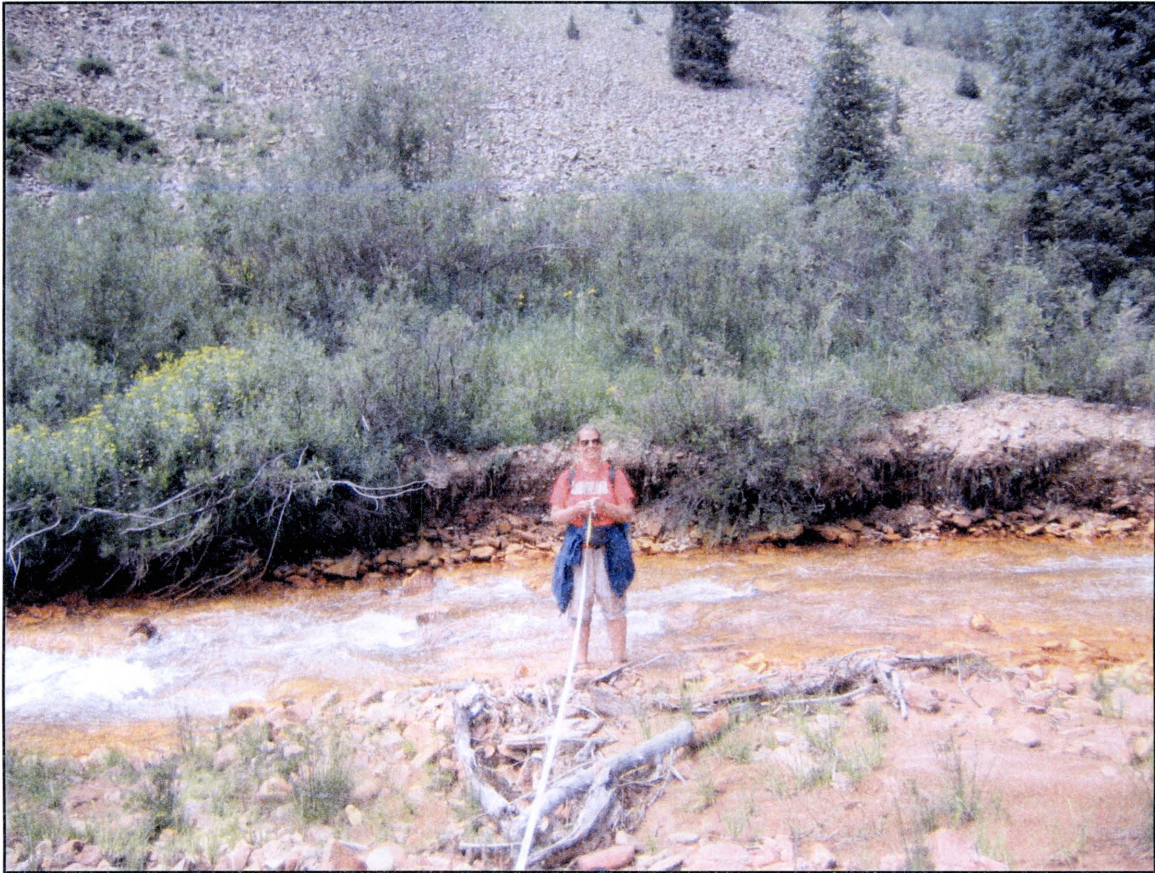
FAIL LENGTH (m)	SIDE	FRAME #	DEPPRESS	ID	LINE	PRINCIPAL POINT
5	R		195		7.5	MINDY

Cement Creek – Reach 37, Failure 2

View of Right Bank from Left Bank

FAIL LENGTH (m)	SIDE	FRAME #	DEPPRESS	ID	LINE	PRINCIPAL POINT
10.8	R		0		11	MINDY

Cement Creek – Reach 38, Failure 1



View of Right Bank from Left Bank.

FAIL LENGTH (m)	SIDE	FRAME #	DEPPRESS	ID	LINE	PRINCIPAL POINT
3.4	R		0		8	MINDY

Cement Creek – Reach 40, Failure 1



Photo i.

FAIL LENGTH (m)	SIDE	FRAME #	DEPPRESS	ID	LINE	PRINCIPAL POINT
12.3	L		165	i	9	BERNIE
				ii	8.7	BERNIE
				iii	17.3	BERNIE



Photo ii.

FAIL LENGTH (m)	SIDE	FRAME #	DEPPRESS	ID	LINE	PRINCIPAL POINT
12.3	L		165	i	9	BERNIE
				ii	8.7	BERNIE
				iii	17.3	BERNIE



Photo iii.

FAIL LENGTH (m)	SIDE	FRAME #	DEPPRESS	ID	LINE	PRINCIPAL POINT
12.3	L		165	i	9	BERNIE
				ii	8.7	BERNIE
				iii	17.3	BERNIE

Cement Creek – Reach 43, Failure 1



View of Left Bank from Right Bank.

FAIL LENGTH (m)	SIDE	FRAME #	DEPPRESS	ID	LINE	PRINCIPAL POINT
4.8	L		160		10.2	BERNIE

Cement Creek – Reach 44, Failure 1



View of Right Bank from Left Bank.

FAIL LENGTH (m)	SIDE	FRAME #	DEPPRESS	ID	LINE	PRINCIPAL POINT
5.8	R		165		7.9	MINDY

Cement Creek – Reach 45, Failure 1



Photo i.

FAIL LENGTH (m)	SIDE	FRAME #	DEPPRESS	ID	LINE	PRINCIPAL POINT
18.4	R		145	i	8.2	MINDY
			145	ii	6.2	MINDY



Photo ii.

FAIL LENGTH (m)	SIDE	FRAME #	DEPPRESS	ID	LINE	PRINCIPAL POINT
18.4	R		145	i	8.2	MINDY
			145	ii	6.2	MINDY

Cement Creek – Reach 46, Failure 1

View of Right Bank from Left Bank.

FAIL LENGTH (m)	SIDE	FRAME #	DEPPRESS	ID	LINE	PRINCIPAL POINT
8	R		165		3.7	MINDY

Cement Creek – Reach 49, Failure 1



View of Right Bank from Left Bank.

FAIL LENGTH (m)	SIDE	FRAME #	DEPRESS	ID	LINE	PRINCIPAL POINT
9.3	R		150		7.7	BERNIE

Cement Creek – Reach 54, Failure 1

View of Left Bank from Right Bank.

FAIL LENGTH (m)	SIDE	FRAME #	DEPPRESS	ID	LINE	PRINCIPAL POINT
23.7	L		190		12	MINDY

Cement Creek – Reach 54, Failure 2

View of Right Bank from Left Bank.

FAIL LENGTH (m)	SIDE	FRAME #	DEPPRESS	ID	LINE	PRINCIPAL POINT
16.5	R		170		16.9	MINDY

Cement Creek – Reach 57, Failure 1



Photo i.

FAIL LENGTH (m)	SIDE	FRAME #	DEPRESS	ID	LINE	PRINCIPAL POINT
19.5	R		170	i	9.3	MINDY
			150	ii	9	MINDY
			145	iii	9.6	MINDY
			155	iv	9.6	MINDY
			180	v	9.3	MINDY

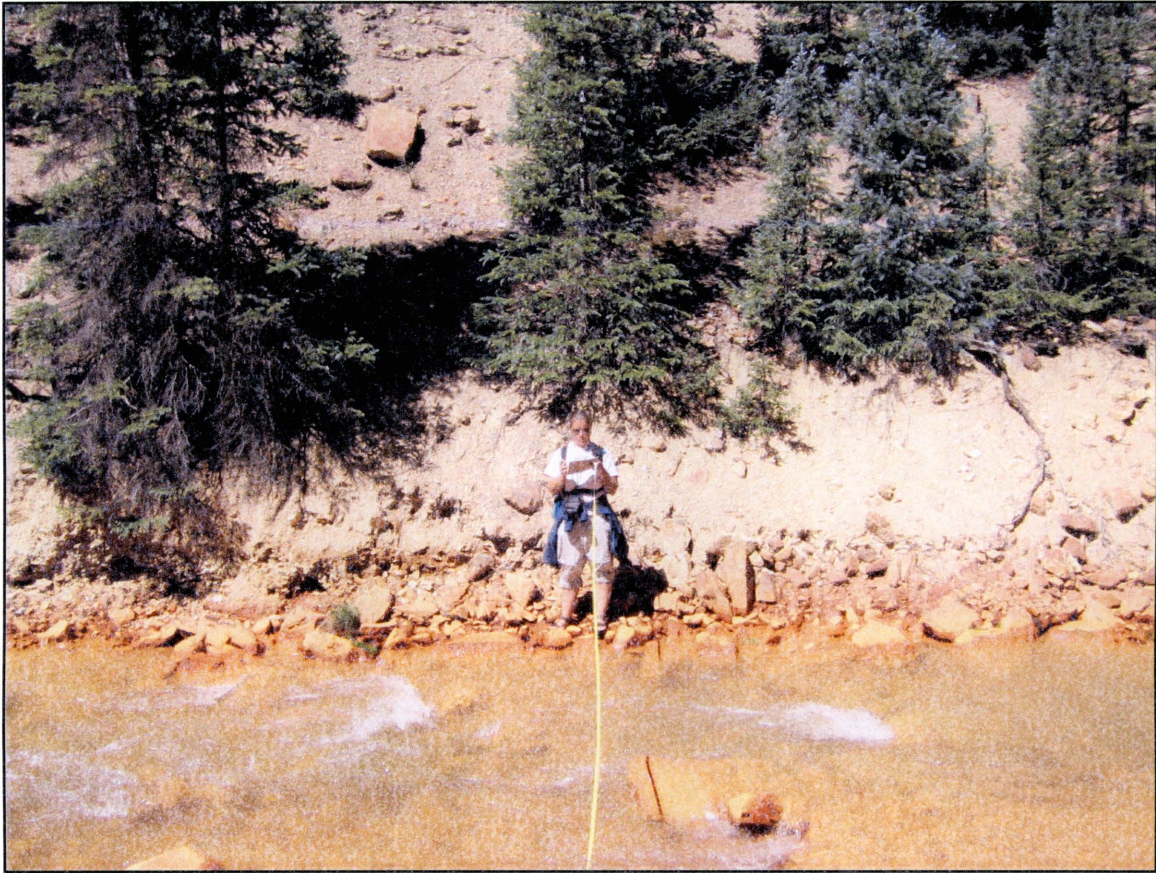


Photo ii.

FAIL LENGTH (m)	SIDE	FRAME #	DEPPRESS	ID	LINE	PRINCIPAL POINT
19.5	R		170	i	9.3	MINDY
			150	ii	9	MINDY
			145	iii	9.6	MINDY
			155	iv	9.6	MINDY
			180	v	9.3	MINDY



Photo iii.

FAIL LENGTH (m)	SIDE	FRAME #	DEPPRESS	ID	LINE	PRINCIPAL POINT
19.5	R		170	i	9.3	MINDY
			150	ii	9	MINDY
			145	iii	9.6	MINDY
			155	iv	9.6	MINDY
			180	v	9.3	MINDY

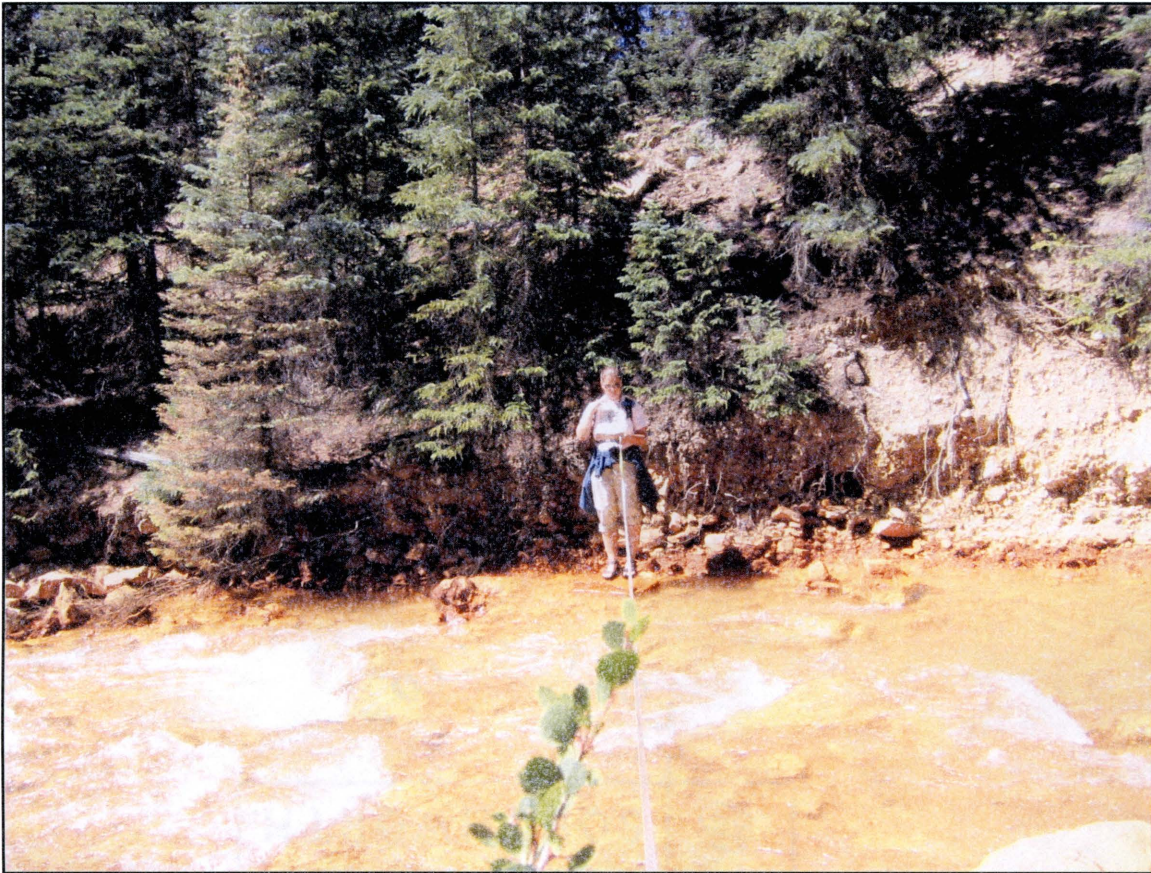


Photo iv.

FAIL LENGTH (m)	SIDE	FRAME #	DEPPRESS	ID	LINE	PRINCIPAL POINT
19.5	R		170	i	9.3	MINDY
			150	ii	9	MINDY
			145	iii	9.6	MINDY
			155	iv	9.6	MINDY
			180	v	9.3	MINDY



Photo v.

FAIL LENGTH (m)	SIDE	FRAME #	DEPPRESS	ID	LINE	PRINCIPAL POINT
19.5	R		170	i	9.3	MINDY
			150	ii	9	MINDY
			145	iii	9.6	MINDY
			155	iv	9.6	MINDY
			180	v	9.3	MINDY

Cement Creek – Reach 59, Failure 1



Photo i.

FAIL LENGTH (m)	SIDE	FRAME #	DEPPRESS	ID	LINE	PRINCIPAL POINT
15.4	L		190	i	7.4	TREE BOTTOM
			180	ii	7.9	TREE BOTTOM
			160	iii	8.4	TREE BOTTOM



Photo ii.

FAIL LENGTH (m)	SIDE	FRAME #	DEPPRESS	ID	LINE	PRINCIPAL POINT
15.4	L		190	i	7.4	TREE BOTTOM
			180	ii	7.9	TREE BOTTOM
			160	iii	8.4	TREE BOTTOM



Photo iii.

FAIL LENGTH (m)	SIDE	FRAME #	DEPPRESS	ID	LINE	PRINCIPAL POINT
15.4	L		190	i	7.4	TREE BOTTOM
			180	ii	7.9	TREE BOTTOM
			160	iii	8.4	TREE BOTTOM

Cement Creek – Reach 61, Failure 1



View of Right Bank from Left Bank.

FAIL LENGTH (m)	SIDE	FRAME #	DEPRESS	ID	LINE	PRINCIPAL POINT
6.3	R		180		7.3	WOOD JUTTING OUT

Cement Creek – Reach 63, Failure 1

View of Left Bank from Right Bank.

FAIL LENGTH (m)	SIDE	FRAME #	DEPPRESS	ID	LINE	PRINCIPAL POINT
3.9	L		175		8	GRASS TUFT

Cement Creek – Reach 63, Failure 2



View of Left Bank from Right Bank.

FAIL LENGTH (m)	SIDE	FRAME #	DEPPRESS	ID	LINE	PRINCIPAL POINT
5.4	L		170		13.1	WOOD

Cement Creek – Reach 66, Failure 1



View of Right Bank from Left Bank.

FAIL LENGTH (m)	SIDE	FRAME #	DEPPRESS	ID	LINE	PRINCIPAL POINT
5.8	R		150		6.2	TAPE TIED TO STICK

Cement Creek – Reach 66, Failure 2



View of Right Bank from Left Bank.

FAIL LENGTH (m)	SIDE	FRAME #	DEPPRESS	ID	LINE	PRINCIPAL POINT
5.4	R		160		7.4	MINDY FEET

Cement Creek – Reach 66, Failure 3

View of Right Bank from Left Bank.

FAIL LENGTH (m)	SIDE	FRAME #	DEPPRESS	ID	LINE	PRINCIPAL POINT
10	R		175		11.4	MINDY

Cement Creek – Reach 75, Failure 1

View of Right Bank from Left Bank.

FAIL LENGTH (m)	SIDE	FRAME #	DEPPRESS	ID	LINE	PRINCIPAL POINT
4.5	R		160		5.3	MINDY

Cement Creek – Reach 75, Failure 2



Photo i.

FAIL LENGTH (m)	SIDE	FRAME #	DEPPRESS	ID	LINE	PRINCIPAL POINT
24.9	R		160	i	7	MINDY
			165	ii	7.2	MINDY
			170	iii	6.6	MINDY
			155	iv	9.9	MINDY
			140	v	9.8	MINDY



Photo ii.

FAIL LENGTH (m)	SIDE	FRAME #	DEPPRESS	ID	LINE	PRINCIPAL POINT
24.9	R		160	i	7	MINDY
			165	ii	7.2	MINDY
			170	iii	6.6	MINDY
			155	iv	9.9	MINDY
			140	v	9.8	MINDY



Photo iii.

FAIL LENGTH (m)	SIDE	FRAME #	DEPPRESS	ID	LINE	PRINCIPAL POINT
24.9	R		160	i	7	MINDY
			165	ii	7.2	MINDY
			170	iii	6.6	MINDY
			155	iv	9.9	MINDY
			140	v	9.8	MINDY

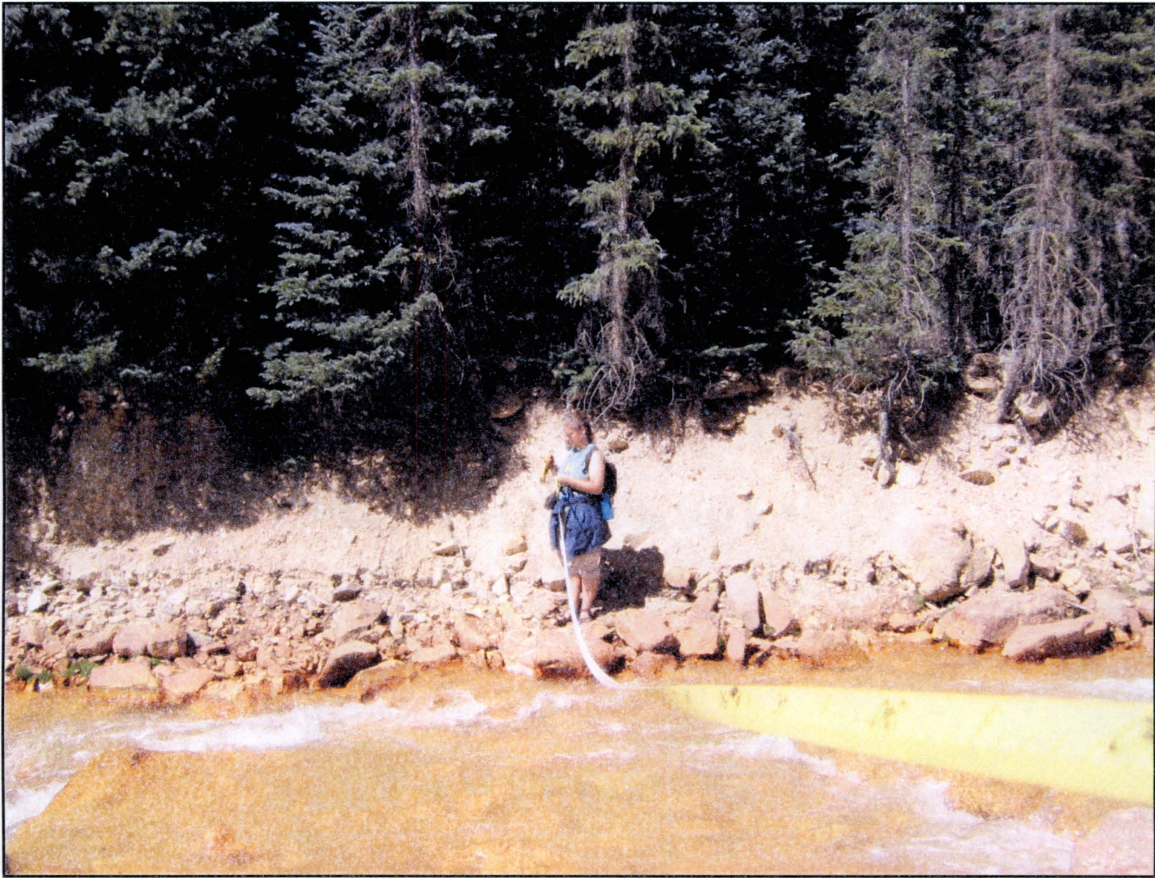


Photo iv.

FAIL LENGTH (m)	SIDE	FRAME #	DEPPRESS	ID	LINE	PRINCIPAL POINT
24.9	R		160	i	7	MINDY
			165	ii	7.2	MINDY
			170	iii	6.6	MINDY
			155	iv	9.9	MINDY
			140	v	9.8	MINDY



Photo v.

FAIL LENGTH (m)	SIDE	FRAME #	DEPPRESS	ID	LINE	PRINCIPAL POINT
24.9	R		160	i	7	MINDY
			165	ii	7.2	MINDY
			170	iii	6.6	MINDY
			155	iv	9.9	MINDY
			140	v	9.8	MINDY

Cement Creek – Reach 76, Failure 1



Photo i.

FAIL LENGTH (m)	SIDE	FRAME #	DEPRESS	ID	LINE	PRINCIPAL POINT
18.1	R		155	i	7.8	MINDY
			155	ii	8	MINDY
			155	iii	8	MINDY
			175	iv	7.5	MINDY
			160	v	8	MINDY



Photo ii.

FAIL LENGTH (m)	SIDE	FRAME #	DEPPRESS	ID	LINE	PRINCIPAL POINT
18.1	R		155	i	7.8	MINDY
			155	ii	8	MINDY
			155	iii	8	MINDY
			175	iv	7.5	MINDY
			160	v	8	MINDY



Photo iii.

FAIL LENGTH (m)	SIDE	FRAME #	DEPPRESS	ID	LINE	PRINCIPAL POINT
18.1	R		155	i	7.8	MINDY
			155	ii	8	MINDY
			155	iii	8	MINDY
			175	iv	7.5	MINDY
			160	v	8	MINDY



Photo iv.

FAIL LENGTH (m)	SIDE	FRAME #	DEPPRESS	ID	LINE	PRINCIPAL POINT
18.1	R		155	i	7.8	MINDY
			155	ii	8	MINDY
			155	iii	8	MINDY
			175	iv	7.5	MINDY
			160	v	8	MINDY



Photo v.

FAIL LENGTH (m)	SIDE	FRAME #	DEPPRESS	ID	LINE	PRINCIPAL POINT
18.1	R		155	i	7.8	MINDY
			155	ii	8	MINDY
			155	iii	8	MINDY
			175	iv	7.5	MINDY
			160	v	8	MINDY

Cement Creek – Reach 76, Failure 2



Photo i.

FAIL LENGTH (m)	SIDE	FRAME #	DEPPRESS	ID	LINE	PRINCIPAL POINT
			170	i	8.6	MINDY
			175	ii	8.2	MINDY
			175	iii	8	MINDY
			190	iv	8.3	MINDY



Photo ii.

FAIL LENGTH (m)	SIDE	FRAME #	DEPPRESS	ID	LINE	PRINCIPAL POINT
			170	i	8.6	MINDY
			175	ii	8.2	MINDY
			175	iii	8	MINDY
			190	iv	8.3	MINDY



Photo iii.

FAIL LENGTH (m)	SIDE	FRAME #	DEPPRESS	ID	LINE	PRINCIPAL POINT
			170	i	8.6	MINDY
			175	ii	8.2	MINDY
			175	iii	8	MINDY
			190	iv	8.3	MINDY



Photo iv.

FAIL LENGTH (m)	SIDE	FRAME #	DEPPRESS	ID	LINE	PRINCIPAL POINT
			170	i	8.6	MINDY
			175	ii	8.2	MINDY
			175	iii	8	MINDY
			190	iv	8.3	MINDY

Cement Creek – Reach 78, Failure 1



Photo i.

FAIL LENGTH (m)	SIDE	FRAME #	DEPRESS	ID	LINE	PRINCIPAL POINT
17	L		168	i	8.4	MINDY
			162	ii	12.1	MINDY
			170	iii	12.2	MINDY
			180	iv	11.6	MINDY



Photo ii.

FAIL LENGTH (m)	SIDE	FRAME #	DEPPRESS	ID	LINE	PRINCIPAL POINT
17	L		168	i	8.4	MINDY
			162	ii	12.1	MINDY
			170	iii	12.2	MINDY
			180	iv	11.6	MINDY



Photo iii.

FAIL LENGTH (m)	SIDE	FRAME #	DEPRESS	ID	LINE	PRINCIPAL POINT
17	L		168	i	8.4	MINDY
			162	ii	12.1	MINDY
			170	iii	12.2	MINDY
			180	iv	11.6	MINDY



Photo iv.

FAIL LENGTH (m)	SIDE	FRAME #	DEPPRESS	ID	LINE	PRINCIPAL POINT
17	L		168	i	8.4	MINDY
			162	ii	12.1	MINDY
			170	iii	12.2	MINDY
			180	iv	11.6	MINDY

Cement Creek – Reach 80, Failure 1

View of Right Bank of Left Bank.

FAIL LENGTH (m)	SIDE	FRAME #	DEPPRESS	ID	LINE	PRINCIPAL POINT
3.4			160		9.9	MINDY

APPENDIX II

MINERAL CREEK BANK FAILURE DATA

The data represented in Appendix I displays the bank failure in Mineral Creek. The abbreviations for the data fields are as follows: FAIL LENGTH is the length of bank failure in meters, SIDE is the left or right bank where it occurs, FRAME #, when available, is the frame number in the camera, DEPRESS is the depression angle of the camera, ID is the number of the photo when there are more than one for a single stretch of failure, LINE is the length in meters between the camera and the principal point, and PRINCIPAL POINT is the center point of the photograph.

Mineral Creek – Reach Number 1 Failure 1



Photo i.

FAIL LENGTH (m)	SIDE	FRAME #	DEPPRESS	ID	PRINCIPAL POINT
13.5	L	37	155	i	MINDY
		38	155	ii	MINDY



Photo ii.

FAIL LENGTH (m)	SIDE	FRAME #	DEPPRESS	ID	PRINCIPAL POINT
13.5	L	37	155	i	MINDY
		38	155	ii	MINDY

Mineral Creek – Reach 3 Failure 1

View of Right Bank from Left Bank.

FAIL LENGTH (m)	SIDE	FRAME #	DEPRESS	ID	PRINCIPAL POINT
11.8	R	39	160		MINDY

Mineral Creek – Reach 7, Failure 1

View of Right Bank from Left Bank.

FAIL LENGTH (m)	SIDE	FRAME #	DEPPRESS	ID	PRINCIPAL POINT
1.8	R	41	170		MINDY

Mineral Creek – Reach 7, Failure 2

View of Left Bank from Right Bank.

FAIL LENGTH (m)	SIDE	FRAME #	DEPPRESS	ID	PRINCIPAL POINT
7.4	L	42	175		MINDY

Mineral Creek – Reach 10, Failure 1



Photo i.

FAIL LENGTH (m)	SIDE	FRAME #	DEPPRESS	ID	PRINCIPAL POINT
12.7	L	43	185	i	MINDY
		44	175	ii	MINDY



Photo ii.

FAIL LENGTH (m)	SIDE	FRAME #	DEPPRESS	ID	PRINCIPAL POINT
12.7	L	43	185	i	MINDY
		44	175	ii	MINDY

Mineral Creek – Reach 10, Failure 2

View of the Left Bank from the Right Bank.

FAIL LENGTH (m)	SIDE	FRAME #	DEPPRESS	ID	PRINCIPAL POINT
2	L	45	200		ROCK

Mineral Creek – Reach 12, Failure 1

View of the Right Bank from Left Bank.

FAIL LENGTH (m)	SIDE	FRAME #	DEPPRESS	ID	PRINCIPAL POINT
6.8	R	46	160		MINDY

Mineral Creek – Reach 13, Failure 1

View of the Right Bank from Left Bank.

FAIL LENGTH (m)	SIDE	FRAME #	DEPPRESS	ID	PRINCIPAL POINT
6.5	R	1	165		MINDY

Mineral Creek – Reach 13, Failure 2

View of Right Bank from Left Bank.

FAIL LENGTH (m)	SIDE	FRAME #	DEPRESS	ID	PRINCIPAL POINT
2.7	R	2	180		MINDY

Mineral Creek – Reach 16, Failure 1



Photo i.

FAIL LENGTH (m)	SIDE	FRAME #	DEPPRESS	ID	PRINCIPAL POINT
21.4	L	3	180	i	MINDY
		4	190	ii	MINDY
		5	170	iii	MINDY



Photo ii.

FAIL LENGTH (m)	SIDE	FRAME #	DEPRESS	ID	PRINCIPAL POINT
21.4	L	3	180	i	MINDY
		4	190	ii	MINDY
		5	170	iii	MINDY



Photo iii.

FAIL LENGTH (m)	SIDE	FRAME #	DEPPRESS	ID	PRINCIPAL POINT
21.4	L	3	180	i	MINDY
		4	190	ii	MINDY
		5	170	iii	MINDY

Mineral Creek – Reach 16, Failure 2

View of Left Bank from Right Bank.

FAIL LENGTH (m)	SIDE	FRAME #	DEPPRESS	ID	PRINCIPAL POINT
4.9	L	7	170		MINDY

Mineral Creek – Reach 16, Failure 3

View of Left Bank from Right Bank.

FAIL LENGTH (m)	SIDE	FRAME #	DEPPRESS	ID	PRINCIPAL POINT
3.6	L	8	190		MINDY

Mineral Creek – Reach 18, Failure 1

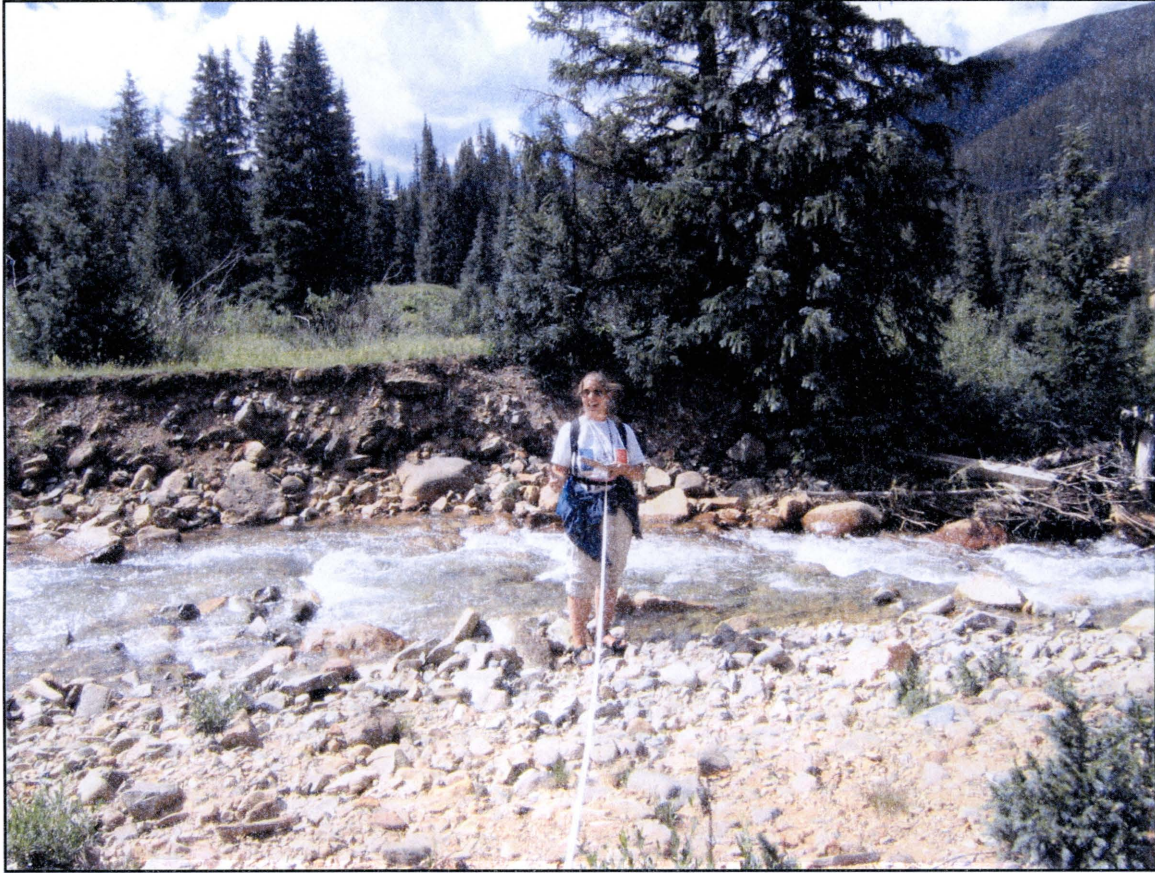
View of Left Bank from Right Bank.

FAIL LENGTH (m)	SIDE	FRAME #	DEPPRESS	ID	PRINCIPAL POINT
9.6	L	9	165		MINDY

Mineral Creek – Reach 20, Failure 1

View of Left Bank from Right Bank.

FAIL LENGTH (m)	SIDE	FRAME #	DEPRESS	ID	PRINCIPAL POINT
4.2	L	10	170		MINDY

Mineral Creek – Reach 32, Failure 1

View of Left Bank from Right Bank.

FAIL LENGTH (m)	SIDE	FRAME #	DEPPRESS	ID	PRINCIPAL POINT
3.3	L	4	150		MINDY

Mineral Creek – Reach 33, Failure 1



Photo i.

FAIL LENGTH (m)	SIDE	FRAME #	DEPPRESS	ID	PRINCIPAL POINT
8.9	L	5	145	i	MINDY
		6	150	ii	MINDY



Photo ii.

FAIL LENGTH (m)	SIDE	FRAME #	DEPPRESS	ID	PRINCIPAL POINT
8.9	L	5	145	i	MINDY
		6	150	ii	MINDY

Mineral Creek – Reach 35, Failure 1

View of Left Bank from Right Bank.

FAIL LENGTH (m)	SIDE	FRAME #	DEPPRESS	ID	PRINCIPAL POINT
4.2	L	7	165		MINDY'S HEAD

Mineral Creek – Reach 36, Failure 1



Photo i.

FAIL LENGTH (m)	SIDE	FRAME #	DEPPRESS	ID	PRINCIPAL POINT
6.8	L	8	170	i	MINDY
		9	190	ii	MINDY



Photo ii.

FAIL LENGTH (m)	SIDE	FRAME #	DEPPRESS	ID	PRINCIPAL POINT
6.8	L	8	170	i	MINDY
		9	190	ii	MINDY

Mineral Creek – Reach 49, Failure 1



Photo i.

FAIL LENGTH (m)	SIDE	FRAME #	DEPRESS	ID	PRINCIPAL POINT
13.2	L	14	180	i	MINDY
		15	175	ii	MINDY



Photo ii.

FAIL LENGTH (m)	SIDE	FRAME #	DEPPRESS	ID	PRINCIPAL POINT
13.2	L	14	180	i	MINDY
		15	175	ii	MINDY

Mineral Creek – Reach 73, Failure 1

Photo i.

FAIL LENGTH (m)	SIDE	FRAME #	DEPRESS	ID	PRINCIPAL POINT
14.2	L	1	175	i	BRANCH W/TAPE
		2	185	ii	BRANCH W/TAPE



Photo ii.

FAIL LENGTH (m)	SIDE	FRAME #	DEPRESS	ID	PRINCIPAL POINT
14.2	L	1	175	i	BRANCH W/TAPE
		2	185	ii	BRANCH W/TAPE

Mineral Creek – Reach 74, Failure 1



Photo i.

FAIL LENGTH (m)	SIDE	FRAME #	DEPPRESS	ID	PRINCIPAL POINT
30.4	L	3	170	i	
		4	180	ii	



Photo ii.

FAIL LENGTH (m)	SIDE	FRAME #	DEPRESS	ID	PRINCIPAL POINT
30.4	L	3	170	i	
		4	180	ii	

Mineral Creek – Reach 75, Failure 1

View Left Bank from Right Bank.

FAIL LENGTH (m)	SIDE	FRAME #	DEPRESS	ID	PRINCIPAL POINT
20	L	5	165		ROCKS AND STICK ON BANK

Mineral Creek – Reach 79, Failure 1



Photo i.

FAIL LENGTH (m)	SIDE	FRAME #	DEPPRESS	ID	PRINCIPAL POINT
24.8	L	6	190	i	TWIG
		7	155	ii	TWIG
		8	170	iii	ROCK



Photo ii.

FAIL LENGTH (m)	SIDE	FRAME #	DEPPRESS	ID	PRINCIPAL POINT
24.8	L	6	190	i	TWIG
		7	155	ii	TWIG
		8	170	iii	ROCK



Photo iii.

FAIL LENGTH (m)	SIDE	FRAME #	DEPPRESS	ID	PRINCIPAL POINT
24.8	L	6	190	i	TWIG
		7	155	ii	TWIG
		8	170	iii	ROCK

Mineral Creek – Reach 88, Failure 1

View of Right Bank from Left Bank.

FAIL LENGTH (m)	SIDE	FRAME #	DEPRESS	ID	PRINCIPAL POINT
5	R	9	160		ROCK

Mineral Creek – Reach 91, Failure 1

View of Left Bank from Left Bank.

FAIL LENGTH (m)	SIDE	FRAME #	DEPPRESS	ID	PRINCIPAL POINT
5.9	L	N/A	N/A	N/A	N/A

Mineral Creek – Reach 93, Failure 1

View of Left Bank from Right Bank.

FAIL LENGTH (m)	SIDE	FRAME #	DEPPRESS	ID	PRINCIPAL POINT
6.4	L	11	165		ROCK

Mineral Creek – Reach 93, Failure 2

Photo i.

FAIL LENGTH (m)	SIDE	FRAME #	DEPPRESS	ID	PRINCIPAL POINT
11	L	12	170	i	ROCK
		13	160	ii	

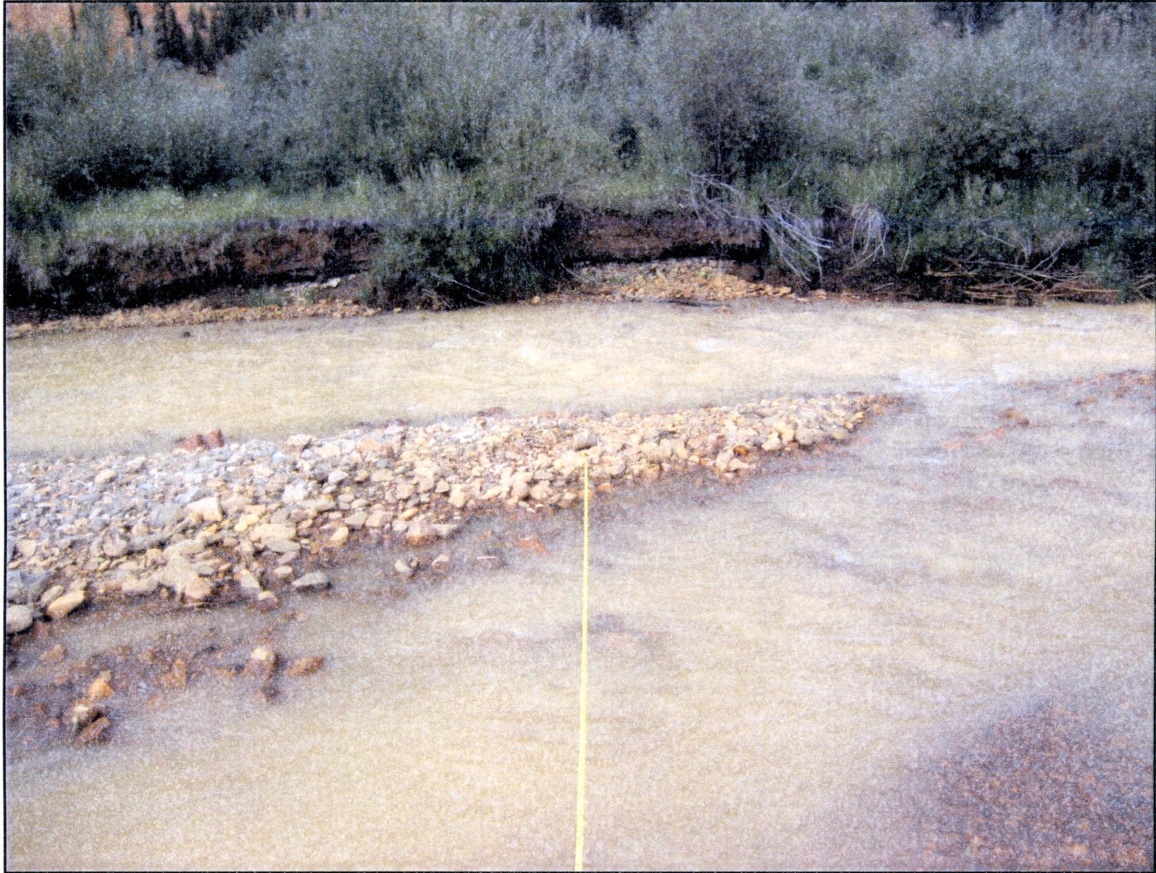


Photo ii.

FAIL LENGTH (m)	SIDE	FRAME #	DEPRESS	ID	PRINCIPAL POINT
11	L	12	170	i	ROCK
		13	160	ii	

Mineral Creek – Reach 99, Failure 1

View of Right Bank from Right Bank.

FAIL LENGTH (m)	SIDE	FRAME #	DEPRESS	ID	PRINCIPAL POINT
2	L	15	205		BURIED WHITE ROCK

Mineral Creek – Reach 100, Failure 1



Photo i.

FAIL LENGTH (m)	SIDE	FRAME #	DEPPRESS	ID	PRINCIPAL POINT
6.2	R	2	200	i	THIN ISOLATED TALL BUSH
		3	215	ii	GRAY ANGLED TWIGS



Photo ii.

FAIL LENGTH (m)	SIDE	FRAME #	DEPPRESS	ID	PRINCIPAL POINT
6.2	R	2	200	i	THIN ISOLATED TALL BUSH
		3	215	ii	GRAY ANGLED TWIGS

Mineral Creek – Reach 101, Failure 1

View of Right Bank from Left Bank.

FAIL LENGTH (m)	SIDE	FRAME #	DEPPRESS	ID	PRINCIPAL POINT
2.8	R	4	155		ORANGE ROCK

APPENDIX III

ALL CEMENT CREEK RESEARCH DATA

Appendix III represents all of the research data utilized in the study for Cement Creek after categorization. The abbreviations for the data fields are as follows: REACH ID is the unique reach number with the lowest number being furthest upstream, PERCENT – R is the percent of failure for the reach on the right bank, PERCENT – L is the percent of failure for the reach on the left bank, FLW indicates if there is presence or absence of fluvial wood detected in the reach with 1 being yes and 0 being no, CLASS – R is the bin failure class for the right bank of the reach, CLASS – L is the bin failure class for the left bank of the reach, and CLASS – ALL, is the bin failure class for both banks of the reach.

REACH ID	PERCENT - R	PERCENT - L	FLW	CLASS - R	CLASS - L	CLASS - ALL
R1	29	18	0	35	25	55
R2	27.5	0	1	35	5	35
R3	3	0	0	5	5	5
R4	9.3	6.9	1	10	10	25
R5	12.7	0	1	15	5	15
R6	20	0	1	25	5	25
R7	0	0	N/A	5	5	5
R8	16.9	0	1	25	5	25
R10	0	3.7	0	5	5	5
R11	0	0	N/A	5	5	5
R12	0	0	N/A	5	5	5
R13	0	0	N/A	5	5	5
R14	0	0	N/A	5	5	5
R15	0	0	N/A	5	5	5
R16	0	0	N/A	5	5	5
R17	0	0	N/A	5	5	5
R18	0	7.5	0	5	10	10
R19	0	0	N/A	5	5	5
R20	0	0	N/A	5	5	5
R21	0	0	N/A	5	5	5
R22	0	0	N/A	5	5	5
R23	0	0	N/A	5	5	5
R24	0	0	N/A	5	5	5
R25	0	0	N/A	5	5	5
R26	9.7	0	1	10	5	10
R27	0	10.2	0	5	15	15
R28	4.9	7.9	1	5	10	15
R29	0	0	N/A	5	5	5
R30	0	0	N/A	5	5	5
R31	0	18	0	5	25	25
R32	0	0	N/A	5	5	5
R33	0	0	N/A	5	5	5
R34	0	2.3	1	5	5	5
R35	0	6.2	1	5	5	5
R36	5.5	0	1	5	10	10
R37	15.8	0	0	25	5	25
R38	3.4	0	1	5	5	5
R39	0	0	N/A	5	5	5
R40	0	12.3	0	5	15	15
R41	0	0	N/A	5	5	5
R42	0	0	N/A	5	5	5
R43	0	4.8	0	5	5	5
R44	5.8	0	1	10	5	10

R45	18 4	0	0	25	5	25
R46	0	3 2	1	5	5	5
R47	0	0	N/A	5	5	5
R48	0	0	N/A	5	5	5
R49	9 3	0	0	10	5	10
R50	0	0	N/A	5	5	5
R51	0	0	N/A	5	5	5
R52	0	0	N/A	5	5	5
R53	0	0	N/A	5	5	5
R54	16 5	23 7	0	25	35	45
R55	0	0	N/A	5	5	5
R56	0	0	N/A	5	5	5
R57	19.5	0	0	25	5	25
R58	0	0	N/A	5	5	5
R59	0	15 4	1	5	25	25
R60	0	0	N/A	5	5	5
R61	6 3	0	0	10	5	10
R62	0	0	N/A	5	5	5
R63	0	9 3	1	5	10	10
R64	0	0	N/A	5	5	5
R65	0	0	N/A	5	5	5
R66	21 2	0	1	25	5	25
R67	0	0	N/A	5	5	5
R68	0	0	N/A	5	5	5
R69	0	0	N/A	5	5	5
R70	0	0	N/A	5	5	5
R71	0	0	N/A	5	5	5
R72	0	0	N/A	5	5	5
R73	0	0	N/A	5	5	5
R74	0	0	N/A	5	5	5
R75	29 4	0	0	35	5	35
R76	18 1	0	1	25	5	25
R77	0	0	N/A	5	5	5
R78	0	17	0	5	25	25
R79	0	0	N/A	5	5	5
R80	3 4	0	0	5	5	5
R81	0	0	N/A	5	5	5
R82	0	0	N/A	5	5	5
R83	0	0	N/A	5	5	5
R84	0	0	N/A	5	5	5
R85	0	0	N/A	5	5	5
R86	0	0	N/A	5	5	5
R87	0	0	N/A	5	5	5
R88	0	0	N/A	5	5	5
R89	0	0	N/A	5	5	5
R9	0	0	N/A	5	5	5
R90	0	0	N/A	5	5	5

R91	0	0	N/A	5	5	5
R92	0	0	N/A	5	5	5
R93	0	0	N/A	5	5	5
R94	0	0	N/A	5	5	5
R95	4 6	0	0	5	5	5
R96	0	0	N/A	5	5	5
R97	0	0	N/A	5	5	5
R98	0	0	N/A	5	5	5
R99	0	0	N/A	5	5	5
R100	0	0	N/A	5	5	5
R101	0	0	N/A	5	5	5
R102	0	0	N/A	5	5	5
R103	0	0	N/A	5	5	5
R104	0	0	N/A	5	5	5
R105	0	0	N/A	5	5	5
R106	0	0	N/A	5	5	5
R107	0	0	N/A	5	5	5
R108	0	0	N/A	5	5	5
R109	0	0	N/A	5	5	5
R110	0	0	N/A	5	5	5
R111	0	0	N/A	5	5	5
R112	0	0	N/A	5	5	5

APPENDIX IV

ALL MINERAL CREEK RESEARCH DATA

Appendix IV represents all of the research data utilized in the study for Mineral Creek after categorization. The abbreviations for the data fields are as follows: REACH ID is the unique reach number with the lowest number being furthest upstream, PERCENT – R is the percent of failure for the reach on the right bank, PERCENT – L is the percent of failure for the reach on the left bank, FLW indicates if there is presence or absence of fluvial wood detected in the reach with 1 being yes and 0 being no, CLASS – R is the bin failure class for the right bank of the reach, CLASS – L is the bin failure class for the left bank of the reach, and CLASS – ALL, is the bin failure class for both banks of the reach.

REACH ID	PERCENT - R	PERCENT - L	FLW	CLASS - R	CLASS - L	CLASS - ALL
M1	0	13.5	1	5	15	15
M2	0	0	N/A	5	5	5
M3	11.8	0	1	15	5	15
M4	0	0	N/A	5	5	5
M5	0	0	N/A	5	5	5
M6	0	0	N/A	5	5	5
M7	1.8	0	0	5	5	5
M8	0	7.4	0	5	10	10
M9	0	0	N/A	5	5	5
M10	0	14.7	1	5	15	15
M11	0	0	N/A	5	5	5
M12	6.8	0	0	10	5	10
M13	9.2	0	0	10	5	10
M14	0	0	N/A	5	5	5
M15	0	0	N/A	5	5	5
M16	29.9	0	0	35	5	35
M17	0	0	N/A	5	5	5
M18	0	9.6	0	5	10	10
M19	0	0	N/A	5	5	5
M20	0	4.2	0	5	5	5
M21	0	0	N/A	5	5	5
M22	0	0	N/A	5	5	5
M23	0	0	N/A	5	5	5
M24	0	0	N/A	5	5	5
M25	0	0	N/A	5	5	5
M26	0	0	N/A	5	5	5
M27	0	0	N/A	5	5	5
M28	0	0	N/A	5	5	5
M29	0	0	N/A	5	5	5
M30	0	0	N/A	5	5	5
M31	0	0	N/A	5	5	5
M32	0	3.3	1	5	5	5
M33	0	8.9	1	5	10	10
M34	0	0	N/A	5	5	5
M35	0	4.2	0	5	5	5
M36	0	6.8	0	5	10	10
M37	0	0	N/A	5	5	5
M38	0	0	N/A	5	5	5
M39	0	0	N/A	5	5	5
M40	0	0	N/A	5	5	5
M41	0	0	N/A	5	5	5
M42	0	0	N/A	5	5	5
M43	0	0	N/A	5	5	5

M44	0	0	N/A	5	5	5
M45	0	0	N/A	5	5	5
M46	0	0	N/A	5	5	5
M47	0	0	N/A	5	5	5
M48	0	0	N/A	5	5	5
M49	0	13.2	1	5	15	15
M50	0	0	N/A	5	5	5
M51	0	0	N/A	5	5	5
M52	0	0	N/A	5	5	5
M53	0	0	N/A	5	5	5
M54	0	0	N/A	5	5	5
M55	0	0	N/A	5	5	5
M56	0	0	N/A	5	5	5
M57	0	0	N/A	5	5	5
M58	0	0	N/A	5	5	5
M59	0	0	N/A	5	5	5
M60	0	0	N/A	5	5	5
M61	0	0	N/A	5	5	5
M62	0	0	N/A	5	5	5
M63	0	0	N/A	5	5	5
M64	0	0	N/A	5	5	5
M65	0	0	N/A	5	5	5
M66	0	0	N/A	5	5	5
M67	0	0	N/A	5	5	5
M68	0	0	N/A	5	5	5
M69	0	0	N/A	5	5	5
M70	0	0	N/A	5	5	5
M71	0	0	N/A	5	5	5
M72	0	0	N/A	5	5	5
M73	0	14.2	1	5	15	15
M74	0	30.4	0	25	35	35
M75	0	20	0	5	25	25
M76	0	0	N/A	5	5	5
M77	0	0	N/A	5	5	5
M78	0	0	N/A	5	5	5
M79	0	24.8	0	5	25	25
M80	0	0	N/A	5	5	5
M81	0	0	N/A	5	5	5
M82	0	0	N/A	5	5	5
M83	0	0	N/A	5	5	5
M84	0	0	N/A	5	5	5
M85	0	0	N/A	5	5	5
M86	0	0	N/A	5	5	5
M87	0	0	N/A	5	5	5
M88	5	0	0	5	5	5
M89	0	0	N/A	5	5	5
M90	0	0	N/A	5	5	5

M91	0	10	1	5	10	10
M92	0	0	N/A	5	5	5
M93	0	17.4	1	5	25	25
M94	0	0	N/A	5	5	5
M95	0	0	N/A	5	5	5
M96	0	0	N/A	5	5	5
M97	0	0	N/A	5	5	5
M98	0	0	N/A	5	5	5
M99	0	2	0	5	5	5
M100	6.2	0	0	10	5	5
M101	2.8	0	0	5	5	5
M102	0	0	N/A	5	5	5
M103	0	0	N/A	5	5	5
M104	0	0	N/A	5	5	5
M105	0	0	N/A	5	5	5
M106	0	0	N/A	5	5	5
M107	0	0	N/A	5	5	5
M108	0	0	N/A	5	5	5
M109	0	0	N/A	5	5	5
M110	0	0	N/A	5	5	5
M111	0	0	N/A	5	5	5
M112	0	0	N/A	5	5	5
M113	0	0	N/A	5	5	5
M114	0	0	N/A	5	5	5
M115	0	0	N/A	5	5	5
M116	0	0	N/A	5	5	5
M117	0	0	N/A	5	5	5
M118	0	0	N/A	5	5	5
M119	9.1	0	0	10	0	10
M120	0	0	N/A	5	5	5
M121	0	0	N/A	5	5	5
M122	0	0	N/A	5	5	5
M123	0	0	N/A	5	5	5
M124	0	0	N/A	5	5	5
M125	0	0	N/A	5	5	5
M126	0	0	N/A	5	5	5
M127	0	0	N/A	5	5	5
M128	0	0	N/A	5	5	5
M129	0	0	N/A	5	5	5
M130	0	0	N/A	5	5	5
M131	0	0	N/A	5	5	5

WORKS CITED

- Aegerter, C. M., K. A. Lorinez, M. S. Welling, and R. J. Wijngaaren. 2004. Extremal dynamics and approach to the critical state: experiments on a three dimensional pile of rice. *Physical Review Letters* 92 (5): 058702.
- Angrati, T. R., E. W. Schweiger, D.W. Bolgrien, P. Ismert, and T. Selle. 2005. Bank stabilization, riparian land use and the distribution of large woody debris in a regulated reach of the upper Missouri River, North Dakota, USA. *River Research and Applications* 20 (7): 829-846.
- Bak, P., and M. Paczuski. 1996. Complexity, contingency, and criticality. *Proceedings of the National Academy of Sciences of the United States of America* 92: 6689-96.
- Bak, P., C. Tang, and K. Wiesenfeld. 1987. Self-organized criticality: an explanation of 1/f noise. *Physical Review Letters* 59 (4): 381-84.
- Bak, P., C. Tang, and K. Wiesenfeld. 1988. Self-organized criticality. *Physical Review A* 38 (1): 364-74.
- Birkeland, K. W., and C. C. Landry. 2002. Power-laws and snow avalanches. *Geophysical Research Letters* 29 (11): 49-1-49-3.
- Carlson, J. M., and J. Doyle. 1999. Highly optimized tolerance: a mechanism for power laws in designed systems. *Physical Review E* 60 (2): 1412-27.
- Coulthard, T. J., and M. J. Van De Wiel. 2006. A cellular model of river meandering. *Earth Surface Processes and Landforms* 31: 123-132.
- Dalström, N., and C. Nilsson. 2004. Influence of woody debris on channel structure in old growth and managed forest streams in central Sweden. *Environmental Management* 33 (3): 376-384.
- Dalton, J. B., T. V. King, D. Bove, R. F. Kokaly, R. N. Clark, J. S. Vance, and G. A. Swayze. 2000. *Distribution of acid-generating and acid-buffering minerals in the Animas River Watershed as determined by AVIRIS spectroscopy*. Proceedings from the ICARD 2000 Meeting, Denver, Colorado, May 21-24, 2000. <http://speclab.cr.usgs.gov/PAPERS/animas1999/animas.html> (10 May 2006).

- DeBoer, D. H. 2000. Self-organization in fluvial landscapes: sediment dynamics as an emergent property. *Computers and Geosciences* 27: 995-1003.
- Faillietaz, J., F. Louchet, and J. Grasso. 2004. Two-threshold model for scaling laws of noninteracting snow avalanches. *Physical Review Letters* 93 (20): 208001.
- Faustini, J. M., and J. A. Jones. 2003. Influence of large woody debris on channel morphology and dynamics in steep, boulder-rich mountain streams, western Cascades, Oregon. *Geomorphology* 51: 187-205.
- Fonstad, M., and W. A. Marcus. 2003. Self-organized criticality in riverbank systems. *Annals of the Association of American Geographers* 93 (2): 281-296.
- Gilden, D. L., T. Thornton, and M. W. Mallon. 1995. 1/f noise in human cognition. *Science, New Series* 267 (5205): 1837-39.
- Graf, W. L., and K. Randall. 1998. *A Guidance Document for Monitoring and Assessing of the Physical Integrity of Arizona Streams*. Arizona Department of Environmental Quality, Contract Report 95-0137: 114.
- Griffiths, H. M. 2005. "Bank failure and channel change as self-organized critical systems." MSc. Thesis, Institute of Geography and Earth Sciences, University of Wales Aberystwyth, 2005.
- Haschenburger, J. K. and S. P. Rice. 2004. Changes in woody debris and bed material texture in a gravel-bed channel. *Geomorphology* 60: 241-267.
- Hergarten, S., and H. J. Heugebauer. 2000. Self-organized criticality in two-variable models. *Physical Review E* 61 (3): 2382-85.
- Hooke, J. 2003. River meander behaviour and instability: a framework for analysis. *Transactions of the Institute of British Geographers* 28 (2): 238-58.
- Ikeda, S., G. Parker, and K. Sawai. 1981. Bend theory of river meanders: I. Linear development. *Journal of Fluid Mechanics* 112: 363-377.
- Kloster, M., S. Maslov, and C. Tang. 2001. Exact solution of a stochastic directed sandpile model. *Physical Review E* 63 (2): 026111.
- Lipman, P. W., H. H. Mehnert, C. W. Naeser, R. G. Luedke, and T. A. Steven, 1976. Multiple ages of mid-Tertiary mineralization and alteration in the Western San Juan Mountains, Colorado. *Economic Geology*, 71: 571-588.
- Malamud, B. D., and D. L. Turcotte. 2000. Cellular-automata models applied to

- natural hazards. *Computing in Science and Engineering* 2 (3): 42-51.
- McGarigal, K., W. H. Romme, M. Crist, and E. Roworth, 2001. Cumulative effects of roads and logging on landscape structure in the San Juan Mountains, Colorado. *Landscape Ecology* 16: 327-349.
- Middleton, A. A., and C. Tang. 1995. Self-organized criticality in nonconserved systems. *Physical Review Letters* 74 (5): 742-45.
- Montgomery, D. R., and J. M. Buffington. 1997. Channel-reach morphology in mountain drainage basins. *Geological Society of America Bulletin* 109 (5): 596-611.
- Montgomery, D. R., B. D. Collins, J. M. Buffington, and T. Abbe. 2003. Geomorphic effects of wood in rivers. *American Fisheries Society Symposium*. 37: 21- 47.
- Montgomery, D. R., and H. Piégay. 2003. Editorial: Wood in rivers: interactions with channel morphology and processes. *Geomorphology* 51: 1-5.
- Murray, A. B., and C. Paola. 1994. A cellular model of braided rivers. *Nature* 371 (6492): 54-57.
- Murray, A. B., and C. Paola. 2003. Modeling the effect of vegetation on channel pattern in bedload rivers. *Earth Surface Processes and Landforms* 28: 131-43.
- Piégay, H., and A. M. Gurnell. 1997. Large woody debris and river geomorphological pattern: examples from SE France and S England. *Geomorphology* 19 (1-2): 99-116.
- Richmond, A. D. and K. D. Fausch. 1995. Characteristics and function of large woody debris in sub-alpine Rocky Mountain streams in northern Colorado. *Canadian Journal of Fisheries and Aquatic Sciences* 52 (8): 1789-1802.
- Robinson, R. "Update: Upper Animas River Watershed Abandoned Mine Land Program." 19 January 2000.
<http://www.co.blm.gov/mines/upperanimas/upperanimas.htm> (10 May 2006).
- Sapozhnikov, V. B., and E. Foufoula-Georgiou. 1996. Do the current landscape evolution models show self-organized criticality? *Water Resources Research* 32 (4): 1109-1112.
- Steven, T. A., K. Hon, and M. A. Lanphere, 1995. *Neogene Geomorphic Evolution of the Central San Juan Mountains Near Creede, Colorado*. U.S. Geological Survey Map I-2504, Denver Colorado.

- Stølum, H-H. 1996. River meandering as a self-organization process. *Science*. 271:1710-13.
- _____. 1997. Fluctuations at the self-organized critical state. *Physical Review E* 56 (6): 6710-18.
- _____. 1998. Planform geometry and dynamics of meandering rivers. *Geological Society of America Bulletin* 110 (11): 1485-98.
- Thomas, R., and A. P. Nicholas. 2002. Simulation of braided river flow using a new cellular routing scheme. *Geomorphology* 43: 179-95.
- Wohl, E. 2000. *Mountain Rivers*. Washington, D.C.: American Geophysical Union, 2000.

VITA

Jane B. Heath was born in Houston, Texas on March 17, 1977, the daughter of Diane and Michael Heath. Ms. Heath received a B.A. from the Department of Geography at the University of Texas at Austin with an emphasis in cultural geography in 1999. She has consistently worked in the field of geography beginning in 1998 with an internship at the Texas General Land Office. Upon graduation, she became a GIS technician for Harner and Associates, a demographic consulting firm, assisting with multiple contracts with Texas school districts mapping optimum bus routes through demographic projections gaining database management, GIS, and DOS skills among others. In 2000 Ms. Heath went on to work in the field full-time as a GPS Analyst for the Utility Automation Integrators, a company that creates GIS systems for utility companies. It was not; however, until Ms. Heath began work as the sole GIS Specialist for R. J. Brandes Company, a surface water resources consulting firm, that she formulated greater interest in physical geography and environmental science, particularly in hydrology and the spatial aspects of river system and watershed studies. In August of 2003 she entered the Graduate College of Texas State University-San Marcos.